

WAVE-DOMINATED SHELVES: A MODEL OF SAND-RIDGE FORMATION
BY PROGRESSIVE, INFRAGRAVITY WAVES

by

B. Boczar-Karakiewicz¹ and J.L. Bona²

¹INRS-Océanologie, Université du Québec, 310 Avenue des Ursulines, Rimouski,
Québec, G5L 3A1, Canada

²Department of Mathematics, The University of Chicago, 5734 University Avenue,
Chicago, IL 60637, U.S.A.

ABSTRACT

Sand ridges having longitudinal crests with spacings of hundreds to thousands of meters are observed to form on sediment-laden shelves. The stability of these sandy bodies suggests that they may be time-averaged responses to the complex hydrodynamics of their environment. Consideration of the scales involved seems to indicate that locally-generated storm waves are not responsible for these structures. Such disturbances may indeed modify existing bars, but appear not to contribute essentially to the formation and mean features of sand ridges. On shelves which we shall refer to as "wave-dominated," a mechanism that may account for systems of sand ridges is associated with infragravity waves (waves having periods of 0.5 to 5 minutes).

A description of the formation of bars on shelves by the propagation of infragravity waves is proposed. The surface hydrodynamics is modelled by non-linear, dispersive, shallow-water theory. The wave-induced flux of sediment is calculated using an associated mass-transport velocity. The bed topography is then described via a continuity equation. Such a theoretical description results in a coupled system of nonlinear partial differential equations. This system may be simplified somewhat by using a modal decomposition of the surface wave. The resulting equations are then approximated numerically in order to make quantitative predictions about field situations.

The model has been tested against in situ measurements made on the Atlantic coast of the U.S.A. (the Delmarva and Virginia coastal shelves). The agreement between the predictions and the measurements was sufficiently good to warrant

some confidence in the mechanism inherent in the model's derivation. Specifically, the successive crest-to-crest distances, which in the model depend only on the mean bed slope and the incident wave conditions, agree quite well with measured values. The very long time scale for formation of fully-developed bars that is a property of the model provides an a posteriori indication of the stability of these structures. Moreover, general trends in on-shore transport and in slow ridge migration due to shore retreat can also be predicted using this model.

1. INTRODUCTION

The factors and processes controlling the genesis of a sand-ridge topography on a continental margin are not agreed upon, despite their importance in understanding the Holocene transformation of the shelf surface. This circumstance is perhaps not astonishing considering the variety of competing geophysical mechanisms that may contribute to the formation and maintenance of these large-scale, sand bodies.

The present paper proposes an explanation of sand-ridge formation by infragravity waves (waves having periods of 0.5 to 5 minutes). This model predicts the formation and dynamics of sand ridges, and also explains some of their morphological and sedimentological features. In describing the general hydrodynamical environment, only wave-induced effects are considered, and consequently the results obtained apply only to what we shall call "wave-dominated" shelves. Because of this restriction, model predictions will be compared with in situ measurements reported in field studies on the Atlantic shelf of North America where tidal and other currents appear to have little influence on sedimentation processes (cf. Davies, 1964).

Features of sand ridges on the Atlantic shelf essential to the present study are reviewed in Section 2 and a discussion of infragravity waves is presented in Section 3. The model describing wave-bed interactions is introduced in Section 4. A confrontation of model predictions with field measurements for systems of sand ridges on the Atlantic shelf is discussed in Section 5, leading to a set of preliminary conclusions which are reported in Section 6.

2. SAND RIDGES ON A WAVE-DOMINATED SHELF

The broad, gently sloping surface of the Atlantic shelf of North America is covered by a large variety of bed forms. A dominating feature is linear, long-crested, sand ridges that often form a rhythmical bed topography, a classical example of which is the field covering the Delmarva inner shelf (Swift et al., 1972b; see Figure 1). In some 200 of these bedforms, ranging geographically from Long Island to Florida, there is a striking morphological regularity, and a rather specific sediment size distribution (Duane et al., 1972). Additionally, these ridges appear to persist over decades, despite evidence of a continuous shoreward-directed sediment flux.

An idea of the scales involved and some of the typical features in ridge fields may be extracted from the cross sections of two ridge fields, shown in Figure 2 (False Cape shelf, after Swift et al., 1972a) and Figure 3 (Ocean City shelf, after Swift et al., 1972b). The length between successive crests in these fields runs from several hundred meters to several kilometers. Notice that the spacing between adjacent crests increases systematically in the offshore direction. Moreover, at least in these two examples, the spacing decreases with decreasing mean slope (the mean slope for False Cape is 0.007 and for Ocean City 0.004). While not evident from these cross sections, Figure 4 (from Swift et al., 1972b) shows that the crests and troughs in these ridge fields are aligned roughly parallel to the shelf edge while at the same time generally lying obliquely with respect to the shoreline.

Across a typical shelf platform the sand-ridge topography shows a systematic change in morphology. The most regular ridges are found in the outer-shelf regions,

whilst the inner-shelf area is characterized by more complexity (the appearance of "secondary crests" is seen in Figure 1 in nearer-shore zones). These changes appear to reflect the gradual change in the hydrodynamical regime that generates and maintains these topographies (Swift et al., 1972b, Swift and Field, 1981).

A variety of bedforms (called variously sand waves, megaripples, and so on) coexist with the main ridge and trough topography. These bedforms may be placed in hierarchical association according to their length scales. Of special note are the smallest, the megaripples, which appear morphologically identical with the surf-zone ripples formed by ordinary gravity waves, and so might be construed as evidence for the existence of "megawaves."

Regarding the sediment's grain-size distribution, the study of Swift and Field (1981) on the inner shelf of the Maryland sector has shown a relationship between the grain distribution relative to ridge topography. On the seaward side of a ridge coarser sand is found, whilst finer sediment occupies the shoreward slopes. Thus we may think of the grain-size distribution as being $\pi/2$ out of phase with respect to the ridge topography, as suggested in Figure 5.

The ridge topography on the Atlantic shelf appears to be stable over time scales of years. Storms, as for example that of Ash Wednesday, 1962 (cf. Duane et al., 1972) may have a strong impact on sediment transport and beach erosion locally in time. In this example a strong, shore-face erosion was nearly compensated for by growth in the sand ridges on the nearby shelf floor, so showing large-scale movement of sediment over quite a short temporal period. However, when the ridge system is viewed as a whole, these short-term changes represent very minor

deviations. Thus one might tentatively conclude that sand ridges are responses more to the average hydrodynamical climate rather than products of intense storms or cyclones, many of which are too localized and moving too rapidly to couple effectively with the water mass lying over the shelf (cf. Vincent et al., 1983).

While major changes aren't the rule, over decades impressive departures may occur such as the landward migration of ridges following the slow retreat of the shoreline. An example of this latter phenomenon is shown in Figure 6 (from Swift et al., 1972b). Detailed mappings of the Ocean City area show that the current ridge system has existed in approximately its present location since at least about 1850, with a slight shift of the whole system to the south (Duane et al., 1972). In the False Cape area, comparison of bathymetries from 1922 to 1969 show about a 350 m. movement of the entire system.

Despite the static nature of these ridge systems, there is nevertheless evidence of a considerable shoreward sediment flux. Pilkey and Field (1972) have pursued several lines of inquiry and concluded that beach and estuarine sands on the U. S. A. Atlantic coast are derived in part from the adjacent continental shelf. Even nondeformable substrates appear to be eroded by a vigorous hydrodynamical environment, as heavy minerals have been found in the inner-shelf sands and the sands of coastal barriers. The sediment movement is plausibly attributed to wave action or currents. If, as seems likely, the sediment moves at rates much in excess of that at which the ridges move, one would be tempted to posit that differential rates are involved in the long-term maintenance of the ridges.

It should be candidly admitted that the points we have limned above would not be universally accepted. Indeed, perhaps the only point of general accord is that sand ridges are associated with an abundant sediment supply. How the sediment comes to be on the shelf, the role of the sediment supply and its dispersal on the shelf, and the development of stable structures appears not to be clearly understood. For the case of what we have called a wave-dominated shelf, some of these issues will be discussed on the basis of a theoretical model that couples the surface wave regime dynamically with sediment transport and bed deformation.

3. INFRAGRAVITY WAVES ON SHELVES

The striking similarity in the external morphology of the linear shoals between Long Island and Florida led Duane et al. (1972) to suggest a common genesis for these sand bodies. They also noted that if their origin lay in storm waves or swell, the existence of large-scale sand ridges in water deeper than 12 - 15 m. would imply wave heights and periods that are unrealistic for the Atlantic coast. Thus whilst it seems plausible that the formation and maintenance of these sand ridges is genetically related to currently active hydrodynamical processes, we must look outside of the range of storm waves and swell for an explanation of their appearance.

As mentioned in Section 2, the megaripples that are found within the main ridge topography may be formed by the well-known instability of a sandy bed subjected to quasi-periodic gravity waves (cf. Boczar-Karakiewicz et al., 1981, and the references contained therein). Whilst the formation of such ripples by gravity waves is not fully understood, one observes as a practical matter that their local spacing, which is typically a small fraction of the surface waves' length, scales with the ratio of surface wavelength to depth. Granting our hypothesis concerning the formation of megaripples on continental shelves, knowledge of their horizontal scales should afford an inference of the wave periods that generated them. Nice examples are found on the Oregon shelf (see Komar et al., 1972) where ripples spaced from 1 to 50 m. apart were observed in depths ranging up to 200 m. A rough-and-ready calculation shows that if the ripples are generated in the manner postulated above, then a nontrivial amount of wave energy must reside in periods from 0.5 to 5.0 minutes.

Such long-period waves, filling the gap in the frequency spectrum between gravity waves and tidal oscillations (see Figure 8), are called infragravity waves. Globally their origin has been loosely linked with wind, very large storm systems, and underwater seismic activity (Kinsman, 1965). Such waves have attracted attention in various contexts, some of which will be described below, but their possible role in inducing sediment movement on continental shelves has been largely neglected.

Munk (1949) observed large-period progressive waves impinging upon the nearshore zone. These waves were termed "surf beats," and it was noted that they appeared to be long-crested, showing no significant longshore variability. Munk and, later, Tucker (1950) attempted an explanation of surf beats in terms of wave groups of long period. The idea was that such groups would have on the whole the same properties, such as breaking and reflection, as a very long-period gravity wave. Following in this line of thought, Longuet-Higgins and Stewart (1962) put forward the view that the additional momentum flux associated with groups of waves results in the depression of the mean surface. This, it was argued, causes a forced wave to travel to the shoreline, where it is assumed to be reflected as a free wave.

The first systematic field measurements of infragravity waves in the near-shore zone with an associated spectral analysis appears to have been effected by Suhayda (1974) in the Arctic. Several peaks in the energy spectrum were found in the period range from 75 to 120 seconds. These oscillations were present at the same frequencies in both fair-weather and storm conditions, though the overall energy in the infragravity range increased during storms.

Further evidence of infragravity waves was found near the North Sea coast of Britain (Huntley, 1976), and off the coast of Nova Scotia (Holman et al., 1978). Huntley found a group of sharp peaks in the wave-velocity spectrum corresponding to periods in the 20- to 100-second range. During the measuring period off the coast of Nova Scotia, the wave regime varied from calm to steady swell to a fully aroused sea (due to hurricane Bell). Spectral analysis again revealed a sharp peak in the energy spectrum at a period of about 100 seconds, persisting over the entire range of ambient conditions.

Field studies by Huntley et al. (1981) off the California coast focussed on wave periods in the 30- to 200-second band. With the swell running at a period of about 14 seconds, a pronounced energy peak was found at its first sub-harmonic frequency, and at a frequency corresponding to a 100-second wave period.

Starting with Gallagher (1971), explanations of the sort of observations cited above have been proposed featuring low-frequency, edge-wave oscillations that are generated by various means in the nearshore zone itself. We point especially to the work of Guza and Davis (1974), Huntley (1976), and Holman and Bowen (1979). Some of the measurements already mentioned above showed pronounced longshore variations, so indicating long-period edge waves as an important aspect of nearshore-zone infragravity waves. The measurements of Huntley et al. (1981) showed onshore-offshore energy levels in the infragravity range considerably in excess of that which would be expected as radiation on the basis of the edge-wave theories, so leading to the presumption of deep-water sources of such waves. The same interpretation was also suggested by Guza and Thornton (1982) in their careful study. Short (1975)

was led to presume the existence of obliquely-arriving, long-period, progressive waves as the generating mechanism of linear nearshore bar systems. He established a correlation between the spacing of bars and the wave lengths observed by Suhayda (1974). Thus despite the success of theories for the generation of long-period oscillations in the nearshore zone itself, there is still evidence of offshore origins for such waves.

An extensive study has been reported recently (Wright, 1982; Wright *et al.*, 1982) that featured measurements on a variety of east-coast, Australian sites. The observations were made in 7.5- to 11-second, moderate-energy swell on different beaches that included steep reflective, flat dissipative, and intermediate slopes. In all types of topography, oscillations at periods a good deal longer than the swell were detected. The shortest of these seemed to appear on highly reflective beaches (these were identified as zero-mode subharmonic edge waves, see Figure 9). The lowest frequencies, corresponding to periods of 40 to 100 seconds, were observed in regimes rather like those that obtain on continental shelves, namely on the flattest, most dissipative beaches (see Figure 10). Moreover, on dissipative shores possessing a bar topography, the infragravity waves were found to be highly resonant with the bottom configuration, a finding that is strongly echoed by the outcome of our analysis.

Two conclusions, for which the foregoing lends some support, are important for our model of sand-ridge formation. The first is that there are progressive infragravity waves propagating shoreward over the continental shelf. In the absence of conclusive measurements well out on the shelf, we have attempted to infer the existence of such waves from nearshore data. This is somewhat tenuous owing to

the more complex infragravity oscillations that are expected in such regions.

Nevertheless, the evidence certainly does not exclude our hypothesis. Presuming this conclusion, the next issue of importance for our model concerns the periods of these waves. Here the situation is perhaps more conclusive. If shoreward-directed infragravity waves are present on a given coastline, then the foregoing evidence points to the period range from 75 to 100 seconds as typical. We take as a working hypothesis that there is significant energy in incoming progressive waves in these periods.

In the next section these two conclusions will be incorporated into a model for sand-ridge formation. In Section 5 predictions stemming from the model will be compared with some field measurements made on the Atlantic shelf of North America.

4. THE MODEL

Interest is now focussed on progressive infragravity waves propagating over a sediment-laden shelf. Because of the extreme length of these waves, they constitute shallow-water waves, and so undergo a change of shape in response to the bottom topography, which takes place on a time scale corresponding to a few wavelengths. As the bed surface is composed of a movable substance, the waves' passage may also have an effect on the bottom topography. This latter influence subsists on very much longer time scales, typically on the order of many thousands of wave periods. As the bed deforms, its effect on the incoming waves is consequently modified. Thus the entire system in view, comprising both the water and bed surfaces, has the possibility of complex self-interaction.

An idealized version of this system will be considered, and a mathematical model developed for the description of this idealization. Suppose that a single-frequency, regular, infragravity wave train having a known constant amplitude propagates shoreward from deep water onto a shelf. Suppose further that the waves are long-crested, that they propagate normal to the shelf edge, and that the shelf does not vary appreciably in the longshore direction, so that both the wave and bed motion in question are sensibly two-dimensional (see again Figure 4). Whilst this idealization is quite restrictive, it is nevertheless known to be approximately valid in interesting laboratory and field situations (Boczar-Karakiewicz *et al.*, 1981; Boczar-Karakiewicz and Bona, 1981). It deserves emphasis that we have assumed the infragravity waves to be generated outside the shelf, or at least near the edge of the shelf, and that they impinge on the shelf essentially as a sinusoidal wavetrain.

As will appear presently, incoming, infragravity waves of more complexity than a sine-wave pattern may be accommodated by our model. (In light of the coarse quality of the data with which one must be content in field situations, more complexity may not always be warranted.) However, the presumption that the waves impinge on the shelf from deeper water seems essential to the detailed development of our conception.

The first step in the modelling procedure is to describe the surface-wave motion over relatively short time scales during which the shelf surface may be assumed to be fixed. Consideration of the scales discussed earlier make it clear that the amplitude \bar{a} may be taken to be small and the wavelength \bar{L} may be taken to be large, compared to the local water depth \bar{h} . Thus the Boussinesq equations,

$$\begin{aligned} q_t + \xi_x + \alpha q q_x &= \frac{1}{3} h^2 q_{xxt} + h h_x q_{xt} + \frac{1}{2} h h_{xx} q_t, \\ \xi_t + [(\alpha \xi + h) q]_x &= 0, \end{aligned} \tag{1}$$

may provide a good approximate description of the wavefield's development. In (1), barred dimensional variables (see Figure 11) have been non-dimensionalized according to the scheme,

$$\begin{aligned} (h, x, z) &= \frac{1}{\bar{H}} (\bar{h}, \bar{x}, \bar{z}), & t &= (g/\bar{H})^{1/2} \bar{t}, \\ \xi &= \frac{1}{\alpha \bar{H}} \bar{\xi}, & q &= \frac{1}{\bar{h} + \bar{\xi}} \int_{-\bar{h}}^{\bar{\xi}} \bar{u} d\bar{z}, \end{aligned} \tag{2}$$

where \bar{H} denotes a characteristic depth (e.g., the depth of the water at the shelf edge), g is the magnitude of the acceleration due to gravity, $\alpha = \bar{a}/\bar{H}$, \bar{x} is the

horizontal coordinate with $\bar{x} = 0$ at the shelf edge, say, \bar{z} is the vertical coordinate with $\bar{z} = 0$ at the undisturbed, free water surface, $\bar{u} = \bar{u}(\bar{x}, \bar{z}, \bar{t})$ is the horizontal component of the velocity field at the point (\bar{x}, \bar{z}) at time \bar{t} , and $\bar{\xi} = \bar{\xi}(\bar{x}, \bar{t})$ is the deviation of the free surface from its equilibrium position at the point \bar{x} at time \bar{t} . Thus q represents a nondimensional, depth-averaged, horizontal velocity.

Because the initial and boundary conditions needed to render (1) well-posed exceed the data one can reasonably expect to be provided in a field situation, it is warranted to pass to a cruder level of approximation. Following Lau and Barcelona (1972), the wave amplitude is represented by a simple modal decomposition of the form,

$$\zeta = \zeta(x, X, t) = \sum_{j=1}^2 a_j(X) \exp(ik_j x - i\omega_j t) + c. c., \quad (3)$$

where X is an independent, long, horizontal variable defined by $X = \beta x$ with $\beta = \bar{H}/\bar{L}$, ω_1 is the frequency of the postulated incoming wavetrain and $\omega_2 = 2\omega_1$ is its second harmonic, k_1 and k_2 are wave numbers associated to ω_1 and ω_2 , respectively, by the linearized dispersion relation for (1), and the complex, order-one amplitudes a_1 and a_2 are taken to vary on the scale of wavelengths, and therefore are dependent only on the long variable X . In (3) and subsequently, *c. c.* stands for the complex conjugate of the quantity just preceding it, so in this case

$$c. c. = \sum_{j=1}^2 a_j^*(X) \exp(i\omega_j t - ik_j x).$$

A similar representation is postulated for q . (Of course, the representation (3) is the truncation of an infinite series. Justification for such a truncation has been

provided previously in Lau and Barcilon (1972), Boczar-Karakiewicz et al. (1981), and Boczar-Karakiewicz and Bona (1981).) Assuming that the principal features of the bottom variation are also gradual, it may also be taken that h is a function $h(X)$ of the long variable X .

When placed in conjunction with the requirements that ζ and q are to satisfy (1), the above hypotheses yield the dispersion relation from which k_1 and k_2 are determined and a coupled pair of ordinary differential equations for the complex amplitudes a_1 and a_2 , viz.,

$$\omega_j^2 = \frac{1}{1 + \frac{1}{3}k_j^2}, \quad j = 1, 2, \quad (4)$$

and

$$\begin{aligned} a_1' &= j_1(X)a_1(X) + \delta_1(X)a_1(X)a_2(X)^*, \\ a_2' &= j_2(X)a_2(X) + \delta_2(X)a_1^2(X), \end{aligned} \quad (5)$$

where j_1 , j_2 , δ_1 and δ_2 are functions of X that are determined solely by the wave parameters ω_j and k_j , $j = 1, 2$, and the known bottom configuration $h(X)$ (see again Lau and Barcilon (1972), or Boczar-Karakiewicz and Bona (1981)). The $*$ denotes complex conjugation. The equations (5), when supplemented with the boundary conditions for a_1 and a_2 at $X = 0$, say, provide an approximate description of the evolution of the waveform ζ and the associated depth-averaged velocity q over a given bed configuration h .

We turn now to the waves' impact on the bed. Still taking the bed location to be fixed and known, and assuming a_1 and a_2 , and thereby ζ and q , to be determined, it is then straightforward to infer an expression for the tangential fluid

velocity at the bed, U_0 , from q via inviscid theory. Once U_0 is predicted, there are several ways of attempting to infer an associated sediment movement. One method which is developed in detail in Boczar-Karakiewicz et al. (1986), is to take the view that U_0 drives a sediment-laden, laminar, viscous boundary layer which, owing to an associated drift velocity, is responsible for a mean transport of sediment mass. The observation that nonlinearity induces a small drift velocity was probably first made by Stokes (1947). It was developed in the context mentioned by Longuet-Higgins (1953) (see also Batchelor (1974, p. 355)). Another possibility would be to take the boundary layer as turbulent (Boczar-Karakiewicz and Chapalain, 1984) or to make use of Bowen's simplification of Bagnold's energetic approach to mass transport (see Bagnold (1963), Bowen (1980), and Tessier and Boczar-Karakiewicz (1984)). These three ideas do not exhaust the possibilities in this aspect of the modelling (see, e.g., Smith (1977)), however the general outcome obtained using any of these suggestions is the same. The results presented in Section 5 were developed from the laminar boundary-layer model. In this case, as for the other models in view, there is adduced a mass transport velocity $U_m = U_m(X, z, \tau)$ in the boundary layer which is a quantity that has been averaged over the fundamental, surface-wave period and so is independent of t , but is assumed to depend on a slow time variable τ that is appropriate to the description of the bottom deformation. The mass transport velocity leads in turn to a total sediment flux Q_m given by

$$Q_m(X, \tau) = \chi \int_0^{\delta} U_m(X, z, \tau) \rho(z) dz$$

where ρ denotes the sediment density in the fluid at height z above the bed, δ is

the effective thickness of the boundary layer, and χ is a constant that incorporates various detailed aspects of the sediment. Of course ρ can be taken to be a function of X and τ as well as of z . The differential movement of the sand is then expressed by the continuity equation

$$\frac{\partial h}{\partial \tau} = \frac{\partial Q}{\partial X} (h, U_0, X). \quad (6)$$

A word concerning the new variable τ is in order here. In all the aforementioned models, the relation between t and τ may be made explicit using the previously introduced scaling parameters α and β . It turns out that

$$t/\tau \cong \chi \cdot O(\alpha^2 \beta^2). \quad (7)$$

In the construction of the turbulent boundary-layer model the constant χ was shown to be closely related to the sediment concentration in the boundary layer. The value of χ , which has been estimated in laboratory and field situations, appears to be scale-dependent (cf. Boczar-Karakiewicz and Chapalain (1984) and Boczar-Karakiewicz et al. (1985)). Extrapolating from laboratory and nearshore values, one would guess that the value of χ relevant to sediment movement on a continental shelf is of order 10^{-3} to 10^{-4} . Thus τ/t is of order 10^{-9} to 10^{-10} , so providing a posteriori justification of the independence of these scales. Note that these rough calculations imply that significant bed movement in response to a changing hydrodynamical environment is to be expected on time scales of a few months to a few years.

The three, coupled equations in (5) and (6) comprise the model for wave-bottom interaction. Notice that the slow temporal variable τ enters only parametrically in equations (5), reflecting the fact that the wave field is assumed to be

insensitive to short-term variation in the bed profile. We take advantage of this aspect in implementing a numerical scheme for these equations. Suppose to be given an initial bed configuration $h_0(X) = h(X, 0)$ and a fixed, incoming, deep-water wave train, say a sine wave train specified by $a_1^0 = a_1(0, \tau) = 1.0$ and $a_2^0 = a_2(0, \tau) = 0.0$. The instantaneous properties of the wave field at $\tau = 0$ for $X > 0$ are predicted via equations (5) using a fourth-order, Runge-Kutta scheme, a method that has proven to be efficient, stable, and accurate (Boczar-Karakiewicz et al., 1986). Once the wave field is determined, a new bed configuration is obtained at time $\tau = \Delta\tau$ by approximately solving equation (6) using a straightforward Euler scheme. With $h = h(X, \Delta\tau)$ in hand, the procedure is reinitiated to obtain a bed profile at $\tau = 2\Delta\tau$, $\tau = 3\Delta\tau$, and so on. In many cases an equilibrium configuration is eventually obtained.

The numerical scheme, briefly described above, turns out to be stable and to converge as the discretization parameters tend to zero. A more detailed account of these ideas is to be found in Boczar-Karakiewicz et al. (1986). In the next section the scheme will be put to test in the context of continental shelves.

5. PREDICTIONS AND COMPARISONS

In this section we explore the general characteristics of solutions of the model presented in Section 4 and make direct comparisons of its predictions with two continental-shelf profiles that feature a classical array of sand ridges.

Turning first to the comparisons, two sand-ridge fields from the Delmarva shelf are considered, one from the False Cape area (Figure 2) and one from the Ocean City sector (Figure 3). The model is initiated without any bed features other than the existing mean slope, estimated from bathymetry to be 0.007 and 0.004 for False Cape and Ocean City, respectively. The incident, infragravity wave train is taken to be of moderate amplitude (the parameter α is set at 0.05) with a period of some 80 seconds (see the extended discussion in Section 2). Such waves are long in comparison to the local depth over the entire shelf platform, and so may in principle be described using our model.

The outcome of these two numerical experiments is presented in Figures 12 and 13. A typical instantaneous wave profile is shown in 12(a) and 13(a). The depiction in 12(b) and 13(b) is the variation of the harmonic amplitudes, $|a_1|$ and $|a_2|$, over the shelf at various times, denoted 0, 1, 2, and 3. In 12(c) and 13(c) the evolution of the initially featureless sloping bed is shown at the same times. Notice that the typical wave profiles, whose amplitudes are enormously exaggerated in comparison with the scale of distance from the shelf edge, become progressively more complex as they propagate into shallower water, an effect that coincides with an increase in the mean relative energy in the second harmonic amplitude. It is also clear from 12(b) and 13(b) that this latter effect becomes more pronounced as the bed deforms in response to the wave regime.

Another important aspect of the evolution of the wave field is the strong oscillation of the first and second harmonic that is superposed upon the mean increase in the second harmonic's energy due to shoaling. As shown in Figures 12(b) and 13(b), energy is exchanged between the wave components in a nearly periodic fashion. The horizontal distance between two successive minima of the second harmonic amplitude $|a_2|$ is referred to as the local repetition length, L_r . The repetition length is typically several wavelengths, and it appears to decrease with the local depth. The repetition length L_r is intimately connected with the spacing of the bars that are observed to form (see 12(c) and 13(c)).

The initial, uniformly sloping bed surface develops gradually under the influence of the imposed wave regime into a system of crests and troughs, as shown in 12(c) and 13(c). Whilst the model predictions of the ridge amplitudes (the full lines in 12(c) and 13(c)) are not in close agreement with the corresponding field measurements (the broken lines in 12(c) and 13(c)), the prediction of horizontal scales is really quite good. A direct numerical comparison of the predicted and observed spacing of ridge crests, shown in 12(c) and 13(c) with the predicted spacing displayed in parentheses under the measured spacing, reveals a relative error in this aspect of only a few percent. Notice that in both cases the horizontal scales in the numerically computed bed form follow the lead of the repetition length L_r in the surface wave. The crest-to-crest scales seem to be slope-dependent with slightly shorter values obtaining over the steeper False Cape shelf. As regards the sand-ridge amplitudes, preliminary evidence indicates that better agreement is obtained if dissipation in the wave is taken into account. Such an improvement is being implemented and will be reported on in due course.

Detailed numerical experiments have been carried out to determine how the bar formation is affected by the initial mean slope. A typical result is illustrated in Figure 14 wherein we see that the number of crests appearing over a given rise in mean bottom level decreases, as does the crest-to-crest spacing, when the mean slope is increased and the other parameters are held fixed. This general trend has been observed many times in the field and laboratory (see the discussion in Section 2).

Slow periodic and nonperiodic changes in the mean water level were found to have a significant influence on the model's dynamics, just as they do for actual ridge systems. The results of a numerical experiment simulating a field situation such as that depicted in Figure 6 is shown in Figure 15. A given primary wave is allowed to build a stable ridge system, as in Figure 15(a). The parameters of the model are then changed to reflect an increase in the mean water level and the numerical integration continued with the previously generated bar system as the initiating bottom configuration. The old system of ridges is rebuilt, as shown in Figure 15(b), to a new final state displayed in 15(c). Compared to the originally built ridge system, the new system has migrated landward following a perceived retreat of the shoreline corresponding to the rising water level. By contrast, small, periodic, water-level oscillations simulating tides do not seem to influence the ridge topography in an essential way. An example in support of this thesis is shown in Figure 16 in which the result of a constant-depth calculation, 16(b), may be contrasted to a similar computation, 16(a), in which the water depth was varied periodically by some 10 percent.

Another interesting issue is concerned with the response of a shelf environment possessing patches of nondeformable substrate, as in Figure 7. A calculation was performed in which the initially featureless sloping bed was taken to be rigid except for a relatively thin uniform layer of sediment. (The condition of rigidity was enforced by setting the sediment flux Q_m equal to zero at points where the depth had reached the level of the nondeformable substrate. In our discrete approximation, this does not preclude the possibility that a bare, rigid bed can be subsequently covered with sediment.) The result of this calculation is shown in Figure 17(b) and contrasted to the outcome of the same calculation in which the entire bed is taken to be deformable, Figure 17(a). With a rigid substrate, the system develops isolated sediment bodies rather than crests and troughs. A similar outcome was witnessed in a laboratory experiment in which a long-period surface wave propagating over a thin layer of sand having an initial slope of 0.005 formed two isolated sand crests separated by a flat trough that was the concrete bed of the channel (see Figure 18).

The present model offers a basis for the observed distribution of sediment sizes on continental shelf ridge systems. As shown in Figure 19, which depicts a numerical experiment starting from a flat, featureless bottom, the ambient boundary-layer velocities take on their maximum values on the seaward face of the ridges whilst their minimum excursions are recorded on the shoreward faces. The largest sediment particles capable of responding to the ambient velocities can be moved onto the upper part of the seaward face, but are stationary elsewhere. Hence a coarser average sediment size will accumulate in this region than elsewhere. This deduction fits the data shown in Figure 5 remarkably well.

Another aspect of the model is that it predicts a continuous, gradual, shoreward-directed flux of sediment. In fact, the mass transport velocity U_m and the sediment flux Q_m are typically both predicted by the model to be everywhere shoreward-directed, whilst the building and maintenance of the ridges subsists on the differential sediment fluxes. In fact, as is shown in Boczar-Karakiewicz et al. (1986), the model possesses a several-parameter family of equilibrium configurations which are attractors in the dynamical systems sense, all of which feature a continuous, shoreward movement of sediment. The long time scale τ is appropriate for the description of this sediment movement, according to the model. Insofar as this time scale is short relative to the slow retreat of the shore, the shelf sediment will move toward the shoreline, so yielding one possible explanation for the appearance of outer-shelf sands in inner-shelf regions and the sands of coastal barriers. Of course it should be acknowledged in this context that reflection from the shore has been ignored in our model. Hence the conclusions just reached need to be applied with caution in inner-shelf areas, or on shelves with considerable mean slope.

We also sought to understand the field reports of resonant responses of infragravity waves to particular bed topographies. In Figure 20 an example of the results of a sequence of experiments using the model are presented. In each of the four cases shown, the incident wave parameters, the constant mean water depth, and the amplitudes of the given bed modulations in cases b, c, and d, were all identical. Figure 20(a) shows a reference calculation over a flat bed, Figure 20(b) shows the same wave over a rapidly modulated bed, Figure 20(c) features a very gradually modulated bottom configuration, whilst the modulation of the bed in 20(d) is tuned

to the repetition length observed over the flat bottom. The surface wave takes little notice of the relatively high frequency and low frequency bed modulations, but it is otherwise with its response to the tuned bed in Figure 20(d), where a marked cascade of energy into the second harmonic is evident. Thus the model indicates that the deformation of periodic long waves propagating in shallow water is not affected significantly by features that recur on a scale very different from the waves' natural repetition length. Hence, on gradually sloping beaches which have stable sandbars like those examined by Wright (1982) and Wright *et al.* (1982), the model explains their presence in terms of the average hydrodynamical environment and so would posit the existence of considerable energy in a particular period range in the wave spectrum, namely, that period that presents a repetition length corresponding to the observed bar spacing. But, as just indicated, such wave periods interact resonantly with the bottom, and so the field observation that this is so provides an added inducement to accept the gist of our model. Similarly, one would expect infragravity waves on, say, the eastern United States continental shelf to interact resonantly with the existing sand ridge fields, though to our knowledge data are lacking to confirm or deny this proposition.

6. CONCLUSIONS

Proposed here is a mechanism for the formation of large-scale sand ridges by long waves (infragravity waves of period some 100 seconds). An example of the comparison between the predictions made using a mathematical model incorporating this mechanism and field data from the Atlantic shelf of North America is presented in Figure 21. Several general conclusions emerge from the present study which we now summarize.

The correlation between predictions and measurements was quite reasonable, especially in light of the coarse quality of the initiating parameters. In particular, the model predicts,

(i) the horizontal distances between subsequent crests in a system of sand ridges are on the order of kilometers, and are several times the local wavelength of the incident train;

(ii) crest-to-crest distances increase gradually with increasing water depth; and

(iii) crest-to-crest distances and the number of crests depend on the local mean slope of the shelf platform, with both increasing with decreasing slope.

General trends that are observed in the long-term sediment budget and the local sediment size distribution are also explained by the model.

(iv) The sediment flux due to the action of long-period waves is determined by the mass transport velocity in the bed boundary layer and, in the absence of significant reflection, is always landward directed. However, quantities of sediment displaced by infragravity waves can only be detected by measurements made over

long time intervals because of the weakness of the instantaneous rates of transport. This contrasts with sediment movement due to local storm events, which, however, are too isolated in space and time and whose duration is too short to account for the overall generation and maintenance of sand-ridge fields.

(v) The sediment distribution is out of phase with the bed topography due to a corresponding phase shift of the horizontal mass transport velocity distribution.

The dynamics of ridge systems is predicted by the model to have the following features.

(vi) The migration of ridge systems in the on- or offshore direction is the response of the bed topography to gradual, permanent changes in the mean water level. In contrast, simulated tidal water-level changes had little effect on the simulated sand ridges.

(vii) The formation, maintenance, and stability of sand ridges on a shelf is related to the specific infragravity wave climate, and it is expected that the mutual interaction will produce a resonance phenomenon characterized by a very substantial increase in the mean energy in the second harmonic component.

The reader will readily appreciate that the model proposed herein is at best only a very rough approximation to reality. Nevertheless, the results presented in Section 5 indicate the predictive power of the model as regards field observations (see also Boczar-Karakiewicz and Bona (1981) and Boczar-Karakiewicz et al. (1984)). These results lend credibility to the tentative assertion that at least in some regimes the formation of stable, ridge-like structures on continental shelf beds are influenced, perhaps strongly, by the sort of wave-bottom interaction whose investigation is reported in the present study.

REFERENCES

- Bagnold, R.A. 1963. Mechanics of marine sedimentation. In: The Sea. (Hill, M.N., ed.) Interscience, New York, v. 3, pp. 507-528.
- Batchelor, G.K. 1974. An Introduction to Fluid Dynamics. Cambridge University Press, London.
- Boczar-Karakiewicz, B. and Bona, J.L. 1981. Über die riffbildung an sandigen küsten durch progressive wellen. Mitteilungen des Leichweiß -Instituts für Wasserbau der Technischen Universität Braunschweig, v. 70, pp. 380-420.
- Boczar-Karakiewicz, B., Bona, J.L. and Chapalain, G. 1985. On sediment transport rates and related time scales for sand bar formation in coastal zones. To appear.
- Boczar-Karakiewicz, B., Bona, J.L. and Cohen, D.L. 1986. Interaction of shallow-water waves and bottom topography. To appear.
- Boczar-Karakiewicz, B. and Chapalain, G. 1984. Sedimentation and bed deformation due to long-wave interactions with a movable bed: turbulent boundary layer model. Internal Report, Institut National de la Recherche Scientifique, Rimouski, Québec, Canada.
- Boczar-Karakiewicz, B., Drapeau, G. and Long, B. 1984. Modélisation des barres sableuses littorales de la partie nord des Iles-de-la-Madeleine. Sciences et Techniques de l'Eau, v. 17, pp. 35-39.
- Boczar-Karakiewicz, B., Paplinska, B. and Winiecki, J. 1981. Formation of sand bars by surface waves in shallow water. Laboratory experiments. Rozprawy Hydrotechniczne, v. 43, pp. 111-125.

- Bowen, A.J. 1980. Simple models of nearshore sedimentation; beach profiles and longshore bars. In: The Coastline of Canada. (McCann, S.B., ed.) Geological Survey of Canada, Ottawa, paper 80-10, pp. 1-11.
- Davies, J.J. 1964. A morphogenic approach to world shorelines. Zeitschrift für Geomorphologie, v. 8, pp. 127-142.
- Duane, D.B., Field, M.E., Meisburger, E.P., Swift, D.J.P. and Williams, S.J. 1972. Linear shoals on the Atlantic inner continental shelf, Florida to Long Island. In: Shelf Sediment Transport: Process and Pattern. (Swift, D.J.P., Duane, D.B., and Pilkey, O.H., eds.) Dowden, Hutchinson and Ross, Inc., Stroudsburg, Pennsylvania, Chap. 22, pp. 447-498.
- Gallagher, B. 1971. Generation of surf beat by non-linear wave interactions. Journal of Fluid Mechanics, v. 49(1), pp. 1-20.
- Guza, R.T. and Davis, R.E. 1974. Excitation of edge waves by waves incident on a beach. Journal of Geophysical Research, v. 79, 1285-1291.
- Guza, R.T. and Thornton, E.B. 1982. Swash oscillations on a natural beach. Journal of Geophysical Research, v. 87, pp. 483-491.
- Holman, R.A., Huntley, D.A. and Bowen, A.J. 1978. Infragravity waves in storm conditions. Proceedings of the 16th Conference on Coastal Engineering. American Society of Civil Engineers, New York, Chap. 23, pp. 268-284.
- Holman, R.A. and Bowen, A.J. 1979. Edge waves on complex beach profiles. Journal of Geophysical Research, v. 84, pp. 6339-6346.
- Huntley, D.A. 1976. Long-period waves on a natural beach. Journal of Geophysical Research, v. 81, pp. 6441-6449.

- Huntley, D.A., Guza, R.T. and Thornton, E.B. 1981. Field observations of surf beat: 1. Progressive edge waves. Journal of Geophysical Research, v. 86, pp. 6451-6466.
- Kinsman, B. 1965. Wind Waves: Their Generation and Propagation on the Ocean Surface. Prentice Hall, Inc., Englewood Cliffs, New Jersey.
- Komar, P.B., Neudeck, R.H. and Kulm, L.D. 1972. Observations and significance of deep-water oscillatory ripple marks on the Oregon continental shelf. In: Shelf Sediment Transport: Process and Pattern. (Swift, D.J.P., Duane, D.B., and Pilkey, O.H., eds.) Dowden, Hutchinson, and Ross, Inc., Stroudsburg, Pennsylvania, Chap. 25, pp. 601-620.
- Lau, J. and Barcelon, A. 1972. Harmonic generation of shallow water waves over topography. Journal of Physical Oceanography, v. 2, pp. 405-410.
- Longuet-Higgins, M.S. 1953. Mass transport in water waves. Philosophical Transactions of the Royal Society of London, Series A, v. 245, pp. 535-581.
- Longuet-Higgins, M.S. and Stewart, R.W. 1962. Radiation stress and mass transport in gravity waves, with applications to surf beats. Journal of Fluid Mechanics, v. 13, pp. 481-504.
- Munk, W.H. 1949. Surf beats. EOS Transactions, American Geophysical Union, v. 30, pp. 849-854.
- Pilkey, O.H. and Field, M.E. 1972. Onshore transportation of continental shelf sediment: Atlantic southeastern United States. In: Shelf Sediment Transport: Process and Pattern. (Swift, D.J.P., Duane, D.B., and Pilkey, O.H., eds.) Dowden, Hutchinson, and Ross, Inc., Stroudsburg, Pennsylvania, Chap. 21, pp. 429-446.

- Short, A.D. 1975. Multiple offshore bars and standing waves. Journal of Geophysical Research, v. 80, pp. 3838-3840.
- Smith, J. Dungan. 1977. Modeling of sediment transport on continental shelves. In: The Sea. (Goldberg, McCave, and O'Brien, eds.) Interscience, New York, v. 6, Chap. 13, pp. 539-577.
- Stokes, G.G. 1847. On the theory of oscillatory waves. Cambridgian Transactions of the Philosophical Society, v. 8, pp. 441-473.
- Suhayda, J.N. 1974. Determining nearshore infragravity wave spectra. International Symposium on Ocean Waves Measurement Analysis, v. 1, pp. 54-63.
- Swift, D.J.P., Holliday, B., Avignone, N. and Shideler, G. 1972a. Anatomy of a shore face ridge system, False Cape, Virginia. Marine Geology, v. 12, pp. 58-84.
- Swift, D.J.P., Koford, J.W., Saulsbury, F.P. and Sears, P. 1972b. Holocene evolution of the shelf surface, central and southern Atlantic shelf of North America. In: Shelf Sediment Transport: Process and Pattern: (Swift, D.J.P., Duane, D.B., and Pilkey, O.H., eds.) Dowden, Hutchinson and Ross, Inc., Stroudsburg, Pennsylvania, Chap. 23, pp. 499-574.
- Swift, D.J.P. and Field, M.E. 1981. Evolution of a classic sand ridge field: Maryland sector, North American inner shelf. Sedimentology, v. 38, pp. 461-482.
- Symonds, G., Huntley, D.A. and Bowen, A.J. 1982. Two-dimensional surf beat: long wave generation by a time-varying breakpoint. Journal of Geophysical Research, v. 87, pp. 492-498.

- Tessier, B. and Boczar-Karakiewicz, B. 1984. On nearshore bars in the Gulf of St. Lawrence: formation, modification and modélisation. Abstract, Annales de l'Association Canadienne-Francais pour l'Avancement des Sciences, 52e Congrès, Québec (to appear in the Proceedings of ACFAS), p. 121.
- Tucker, M.J. 1950. Surf beats: Sea waves of 1 to 5 minute period. Proceedings of the Royal Society of London, Series A, v. 202, pp. 565-573.
- Vincent, C.E., Young, R.A. and Swift, D.J.P. 1983. Sediment transport on the Long Island shoreface, North American Atlantic shelf: Role of waves and currents in shoreface maintenance. Continental Shelf Research, v. 2, pp. 163-181.
- Wright, L.D., Guza, R.T. and Short, A.D. 1982. Dynamics of high-energy dissipative surf zone. Marine Geology, v. 45, pp. 41-62.
- Wright, L.D. 1982. Field observations of long-period, surf-zone standing waves in relation to contrasting beach morphologies. Australian Journal of Marine and Freshwater Research, v. 33, pp. 181-201.

LIST OF FIGURES

- Figure 1. A classical example of a sand ridge field: a section of the Delmarva inner shelf region (after Swift et al., 1972b).
- Figure 2. Location and profiles of a sand ridge field on the Atlantic shelf of North America: False Cape area (after Swift et al., 1972a).
- Figure 3. Location and profiles of a sand ridge field on the Atlantic shelf of North America: Ocean City area (after Swift et al., 1972b).
- Figure 4. Shore-normal and shelf-edge-normal orientations for two sand ridge fields (after Swift et al., 1972b).
- Figure 5. Example of a typical grain-size distribution on sand ridges (after Swift and Field, 1981).
- Figure 6. An example of the slow migration of a sand ridge system on the Atlantic shelf due to the slow retreat of the shoreline (after Swift et al., 1972b).
- Figure 7. An example of a typical field situation where the sand ridge crest lies over a nondeformable substrate (after Pilkey and Field, 1972).
- Figure 8. Schematic representation of the energy contained in the surface waves of the oceans: infragravity wave energy fills the gap between gravity waves and so-called long-period waves (after Kinsman, 1965).
- Figure 9. Typical power spectrum of shore-normal currents on a highly reflective beach (Bracken Beach, Australia, after Wright, 1982).
- Figure 10. Typical power spectrum of shore-normal currents on a highly dissipative beach (Goolwa Beach, S.A., after Wright, 1982).
- Figure 11. Definition sketch for the physical variables of the wave field.

Figure 12. Prediction of the formation of a sand-ridge system by a long-period surface wave for the False Cape area: (a) final surface-wave profile, (b) evolution of the harmonics of the wave profile, (c) comparison of field measurements (broken line) with predictions of the model (solid line). Note the comparison of the measured crest-to-crest distances (numbers in brackets) with those predicted by the model (unbracketed numbers).

Figure 13. Prediction of the formation of a sand-ridge system by a long-period surface wave for the Ocean City area: (a) final surface wave profile, (b) evolution of the harmonics of the wave profile, (c) comparison of field measurements (broken line) with predictions of the model (solid line). Note the comparison of the measured crest-to-crest distances (numbers in brackets) with those predicted by the model (unbracketed numbers).

Figure 14. The model's dependence on the initial mean slope for the wave regime obtaining in the Ocean City area.

Figure 15. "Migration" of a sand-ridge system due to an increase in the mean water level: (a) formation of sand ridges for a constant mean water level χ_0 , (b) rebuilding of the system under an increased water level $\chi_0 + \Delta\chi$, (c) final landward-shifted system of ridges.

Figure 16. Formation of sand ridges: (a) in the presence of an oscillating mean water level (tides), (b) in constant water depth.

Figure 17. Formation of sand ridges: (a) over a fully deformable (sandy) bed, (b) over a nondeformable substrate.

Figure 18. Formation of sand ridges over a nondeformable substrate. Laboratory experiments (after Boczar-Karakiewicz et al., 1981).

Figure 19. Relation of wave transformation, sediment transport, and bed deformation for a long-period, progressive, surface wave.

Figure 20. Effects of bed topographies on a long-period, progressive wave:

(a) horizontal bed, (d) bed undulations "tuned" to the horizontal repetition length scale in the wave, (b) bed oscillations of shorter, and (c) of longer, horizontal length scales than the repetition length, L_t .

Figure 21. Model predictions and field measurements for sand ridge fields on the Delmarva shelf.

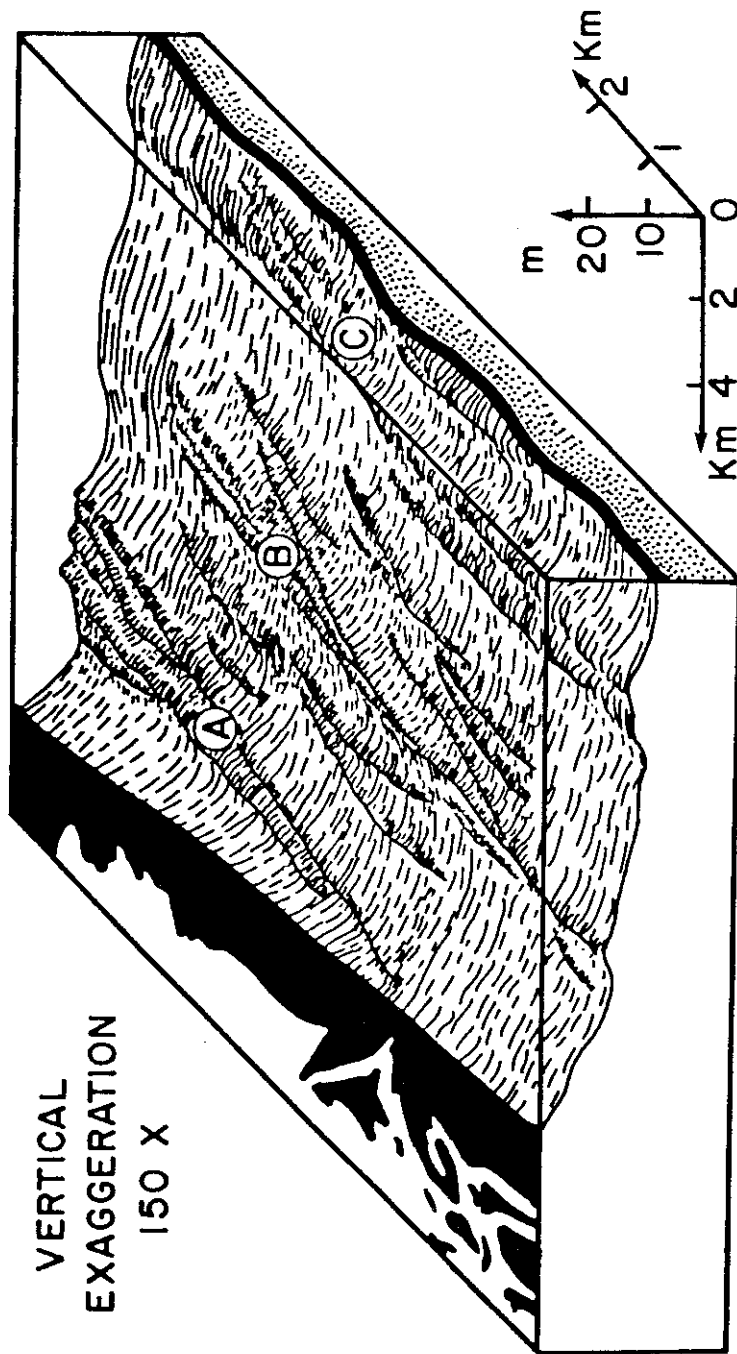


Figure 1.

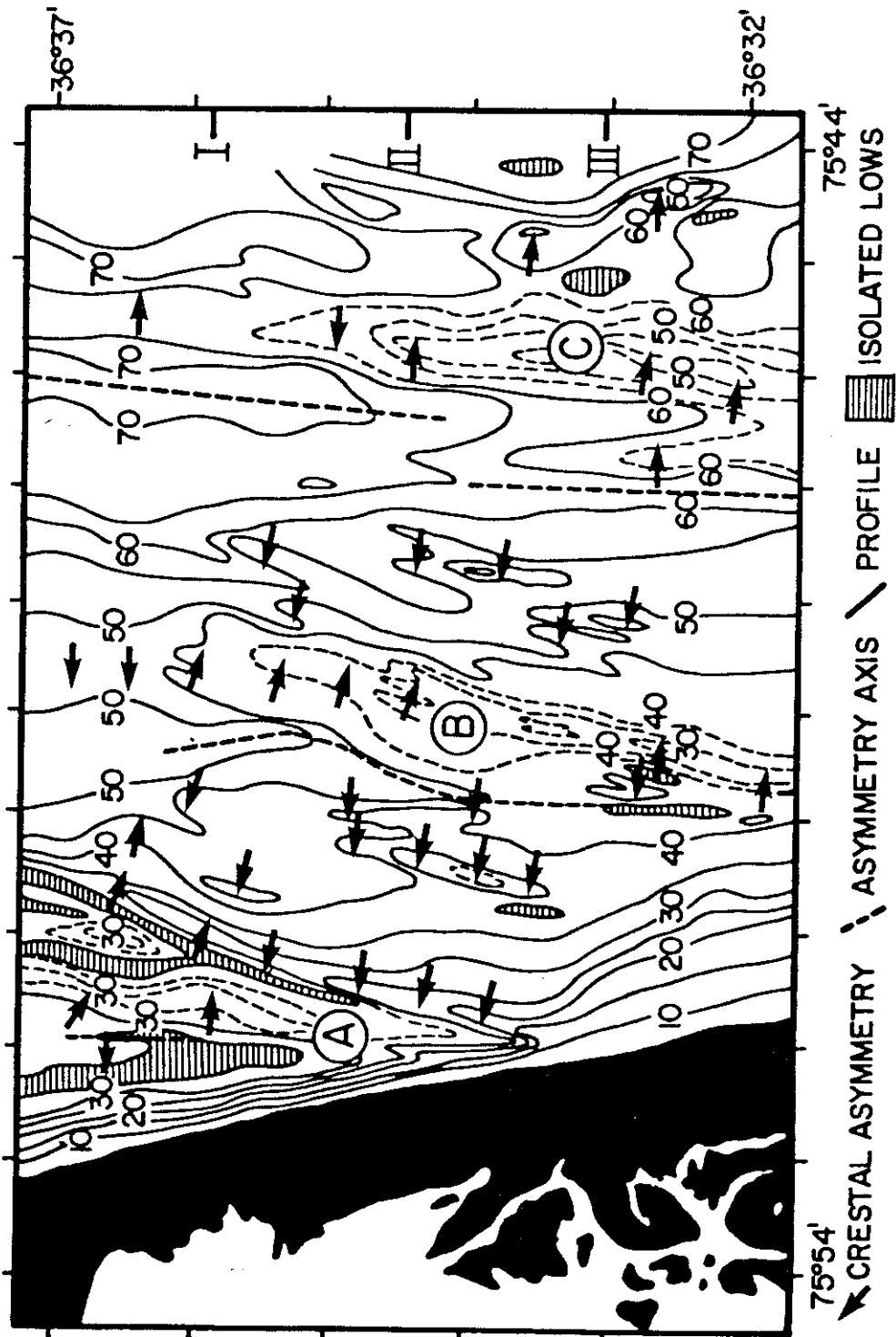


Figure 2.

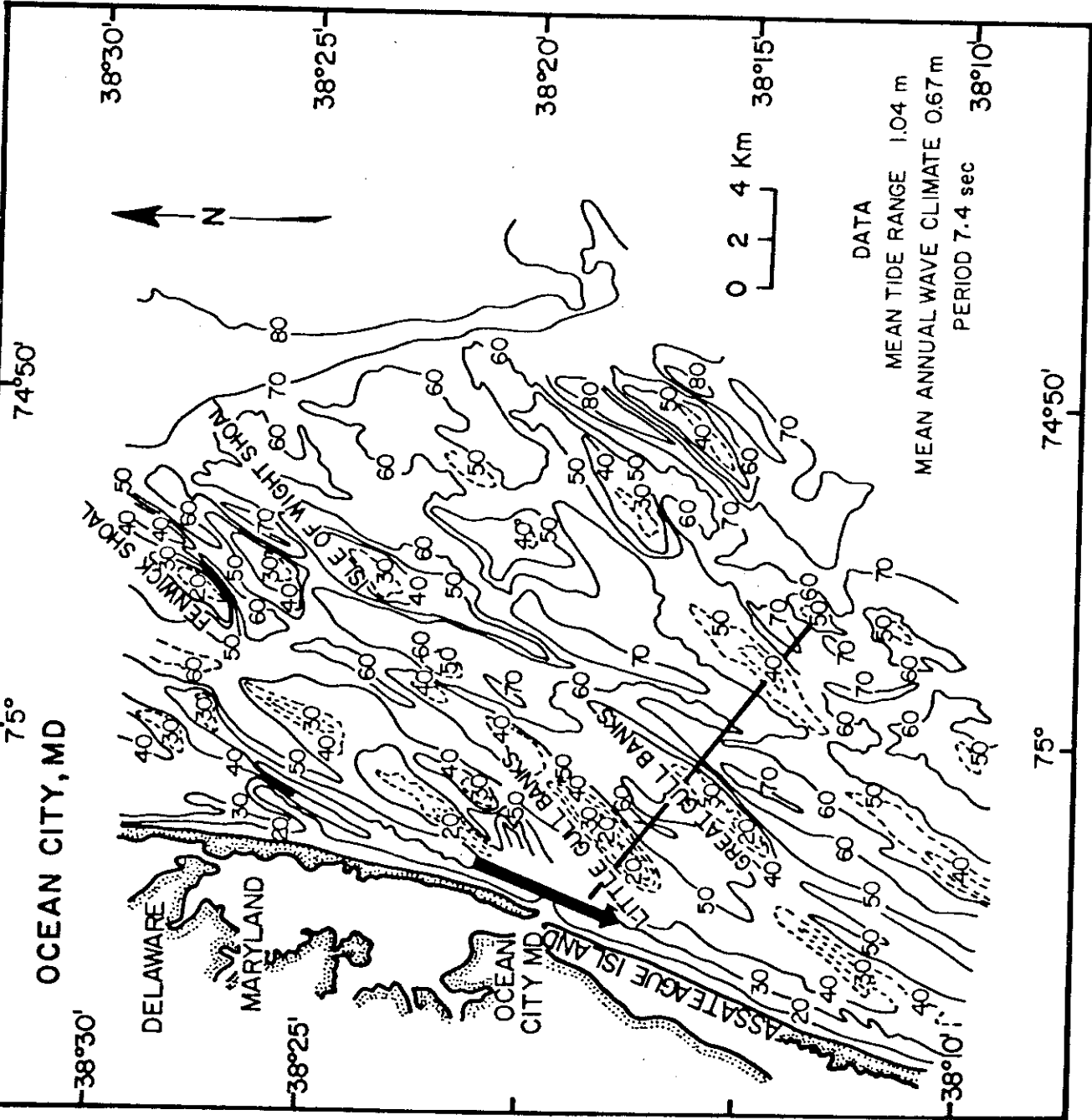


Figure 3.1.

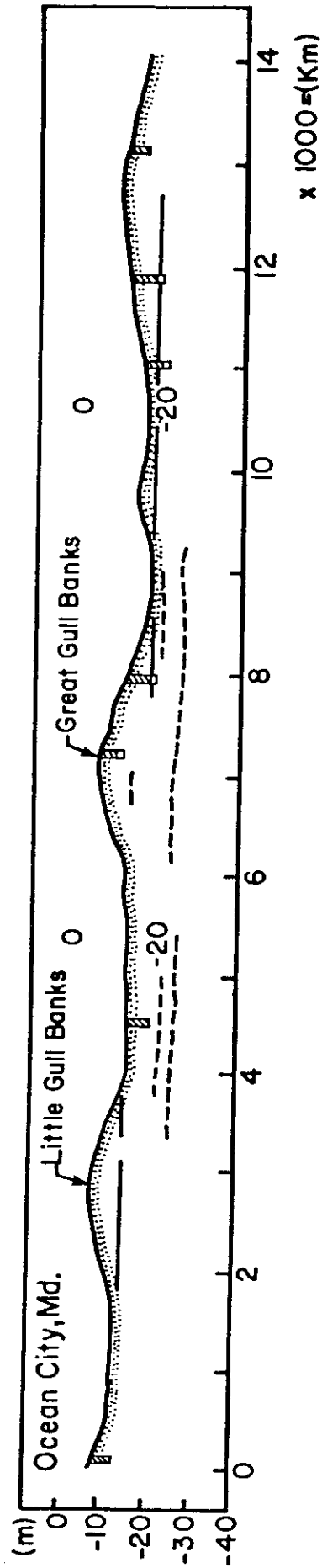


Figure 3.2.

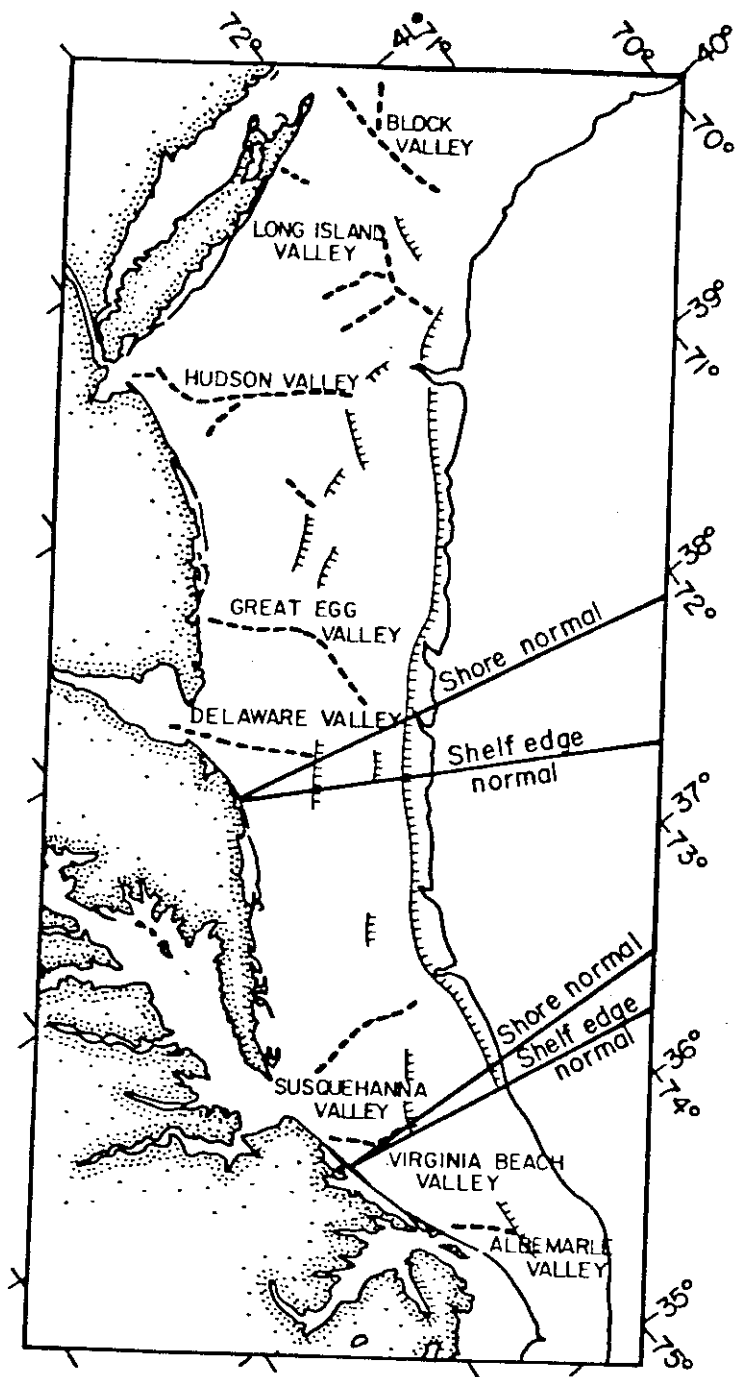


Figure 4.

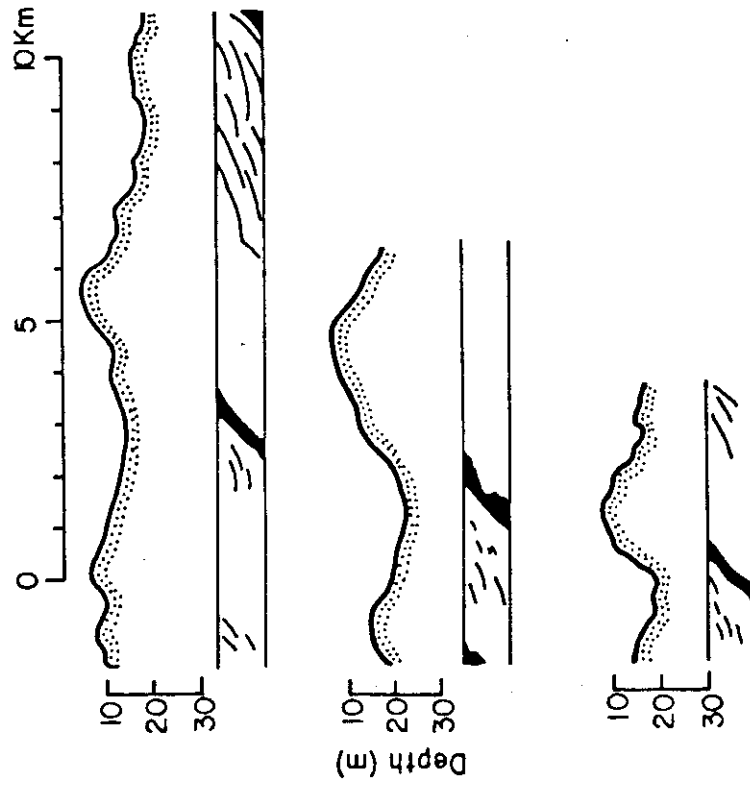


Figure 5.

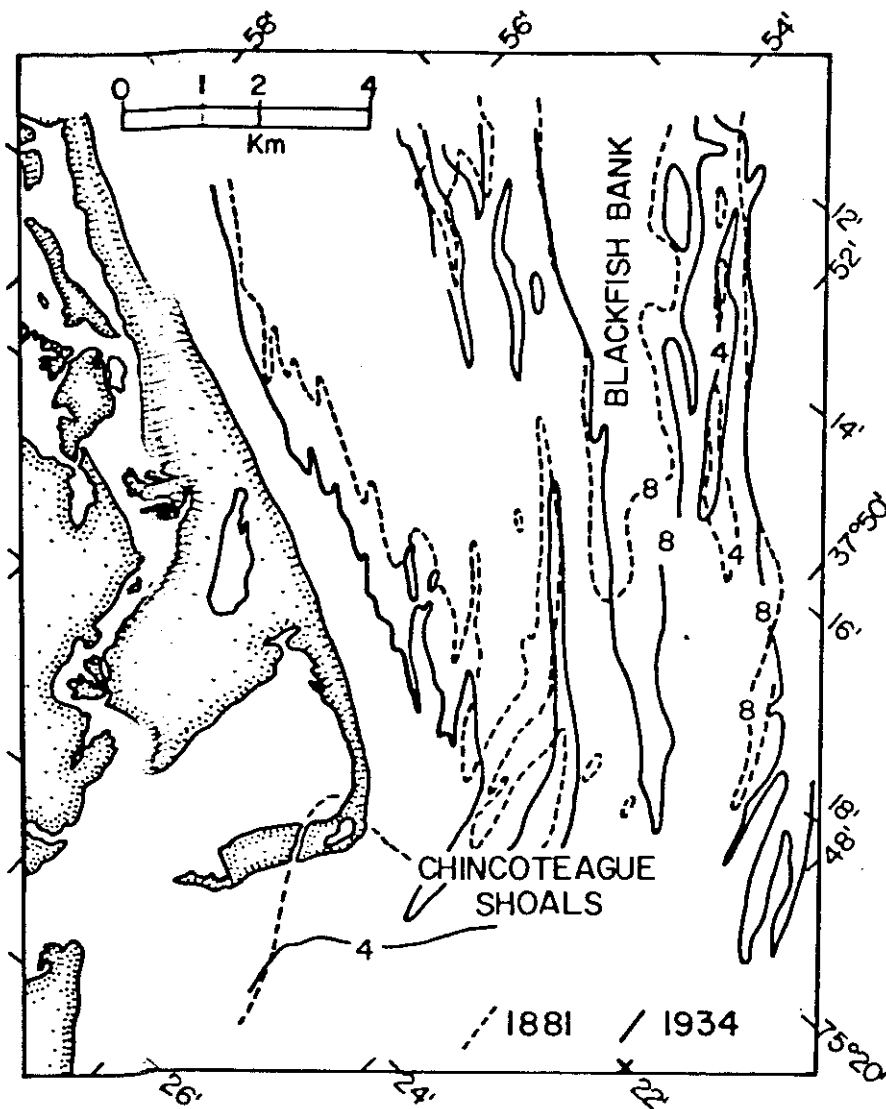


Figure 6.

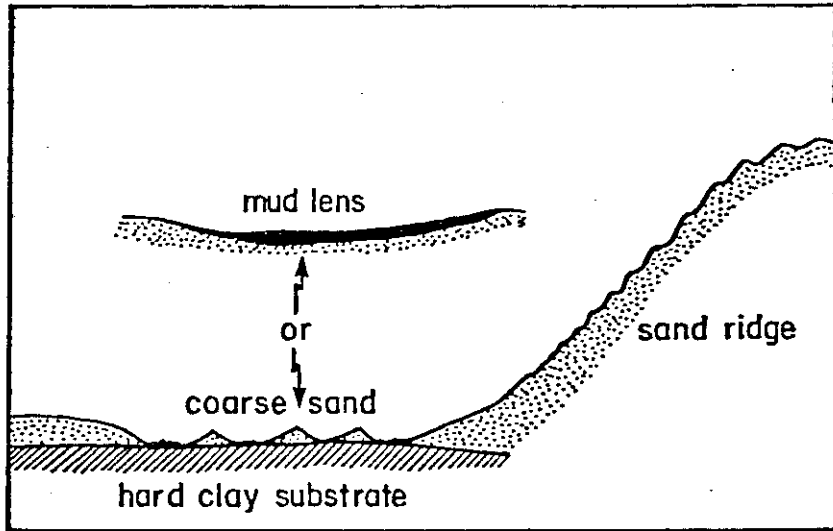


Figure 7.

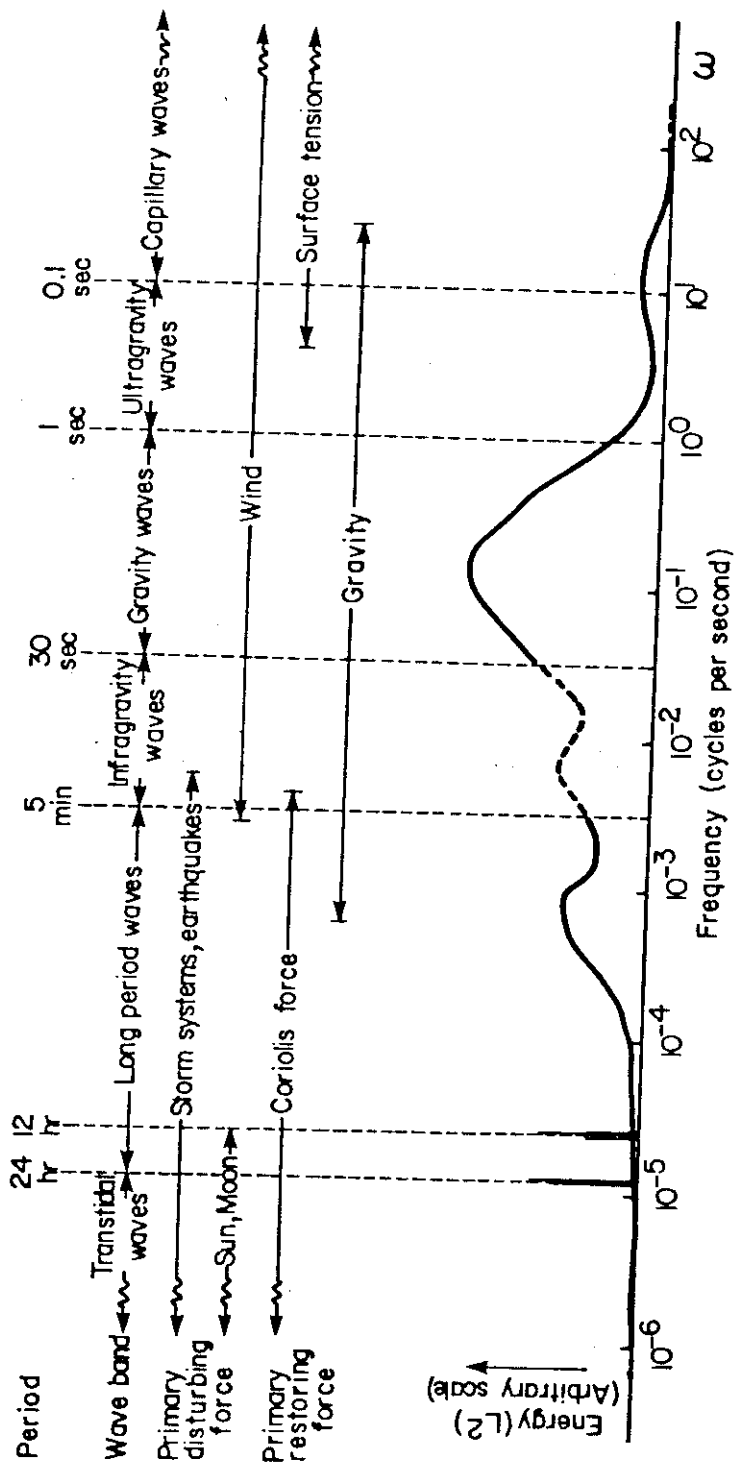


Figure 8.

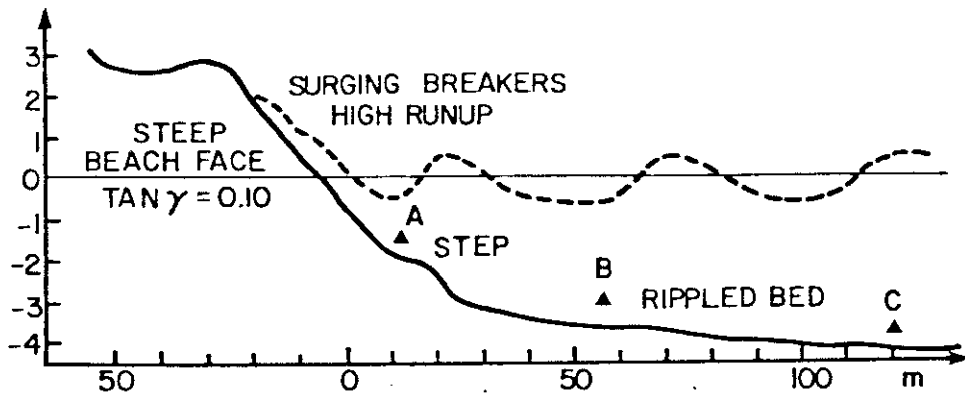
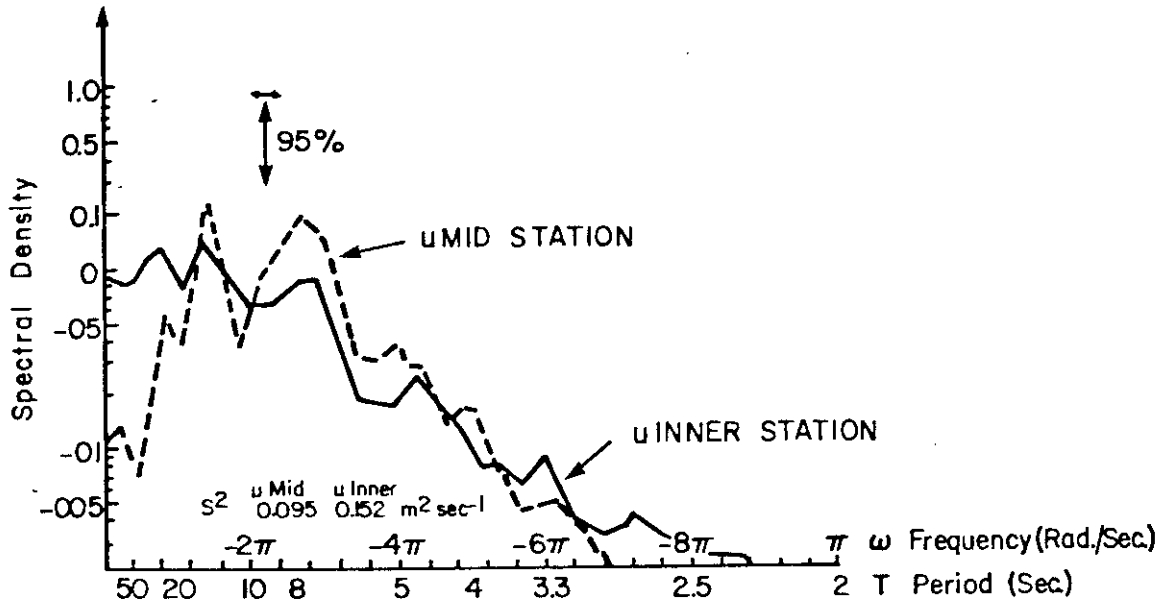


Figure 9.

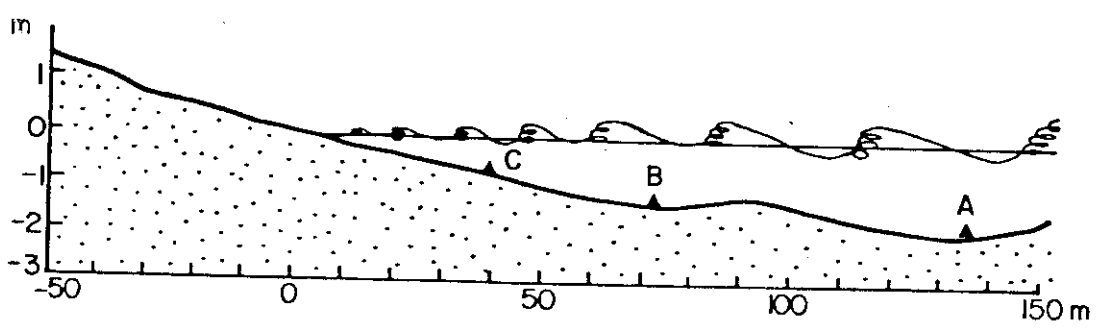
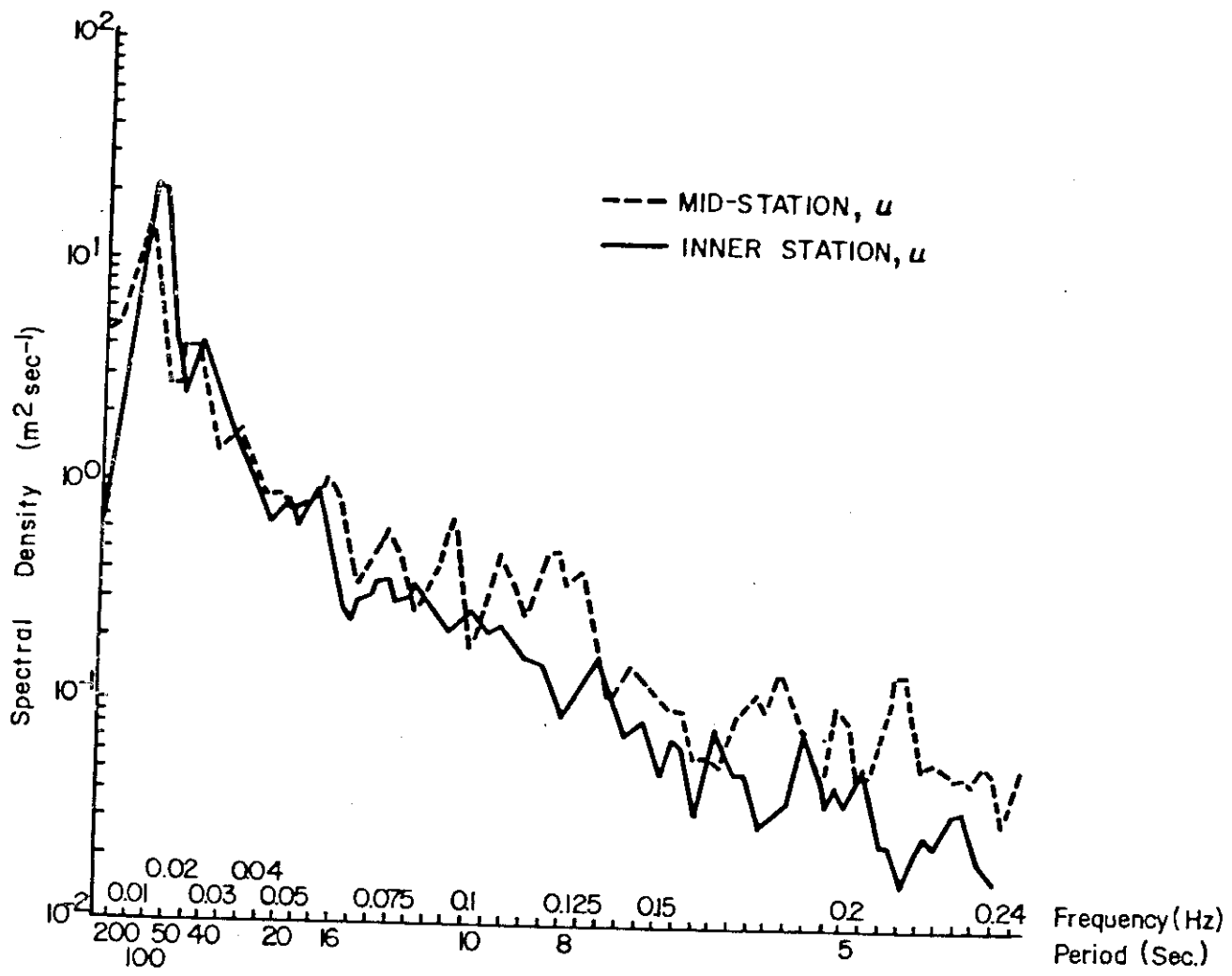


Figure 10

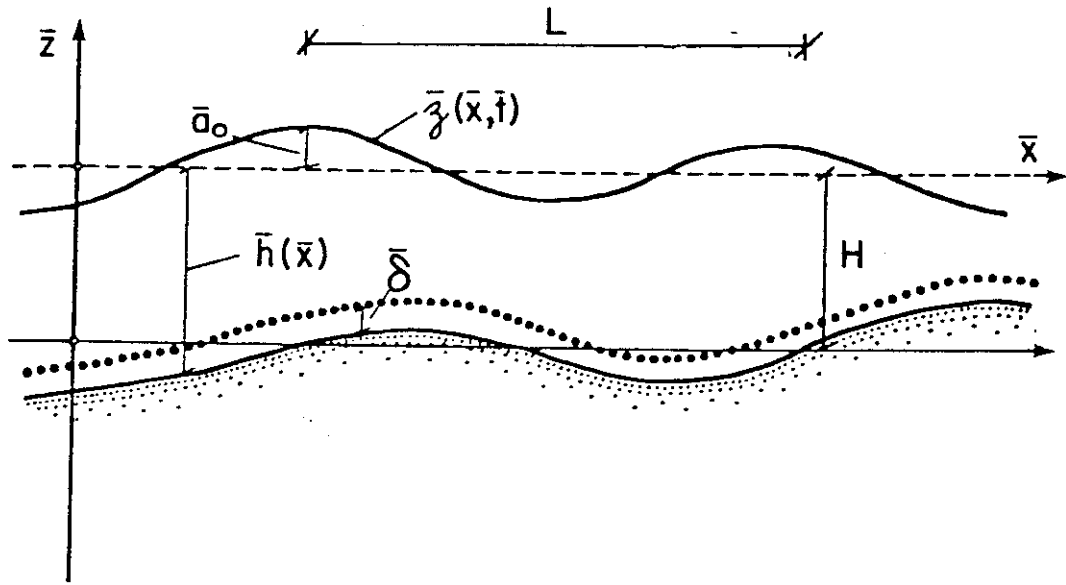


Figure 11.

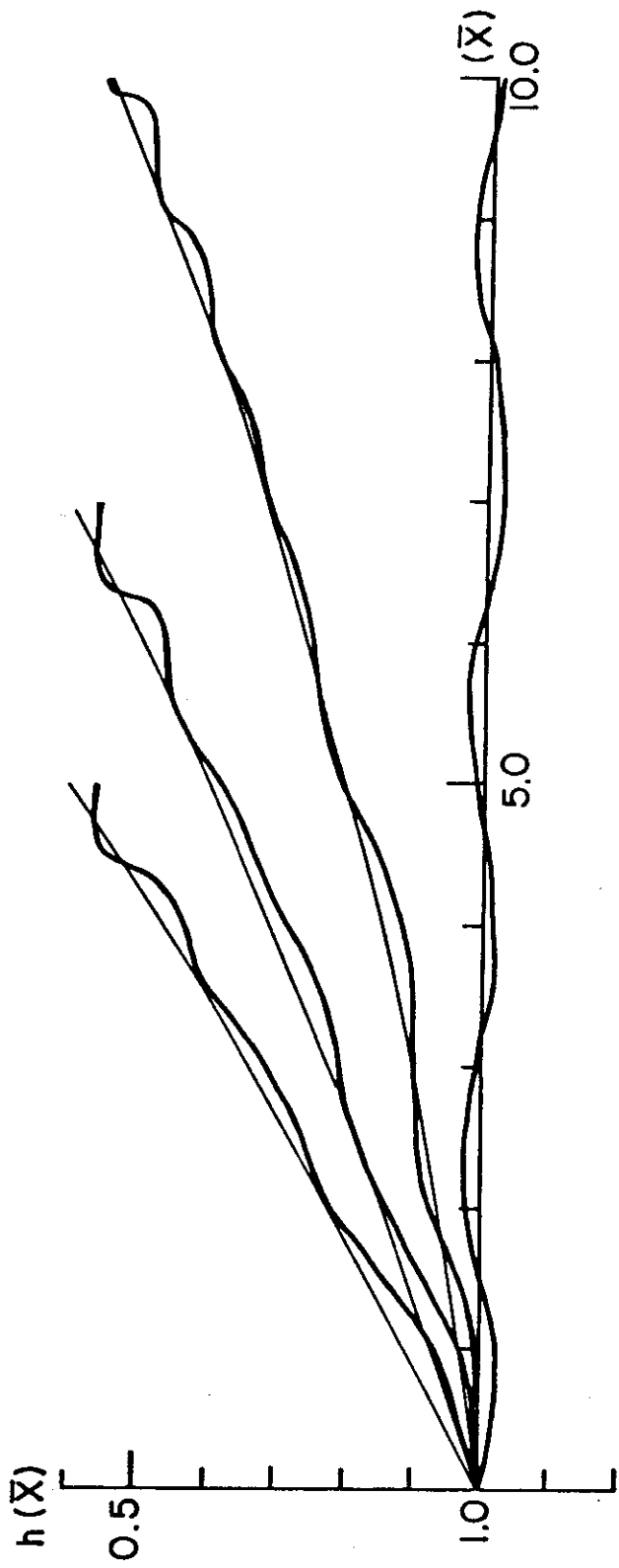


Figure 14.

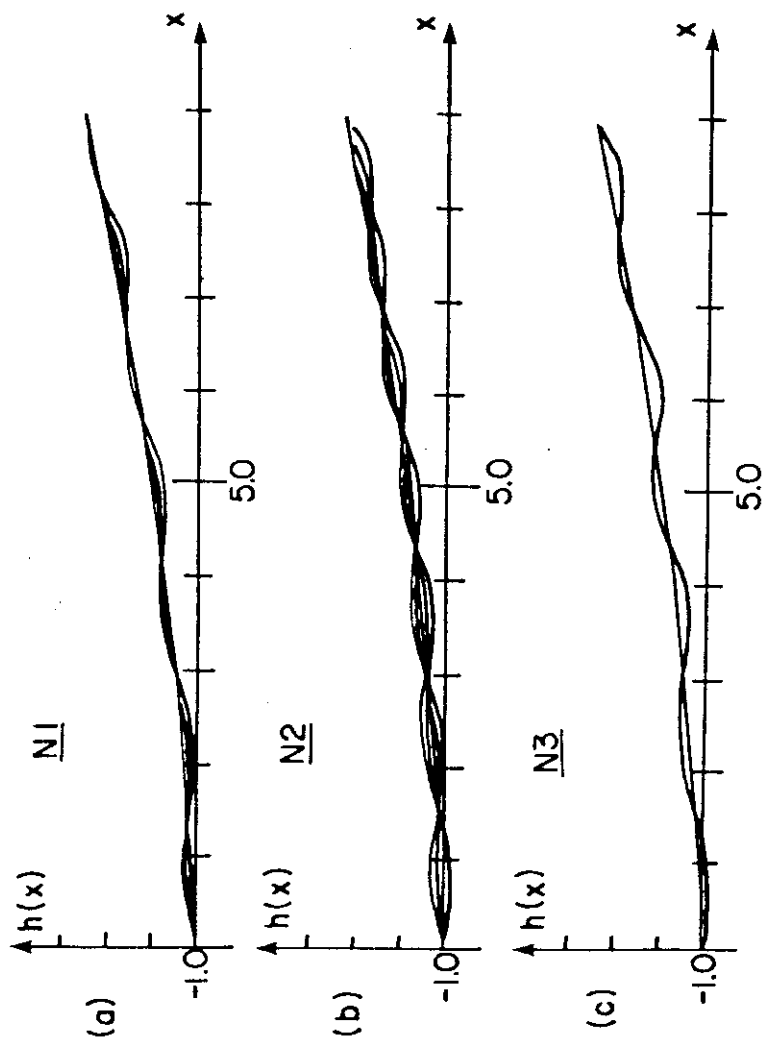


Figure 15.

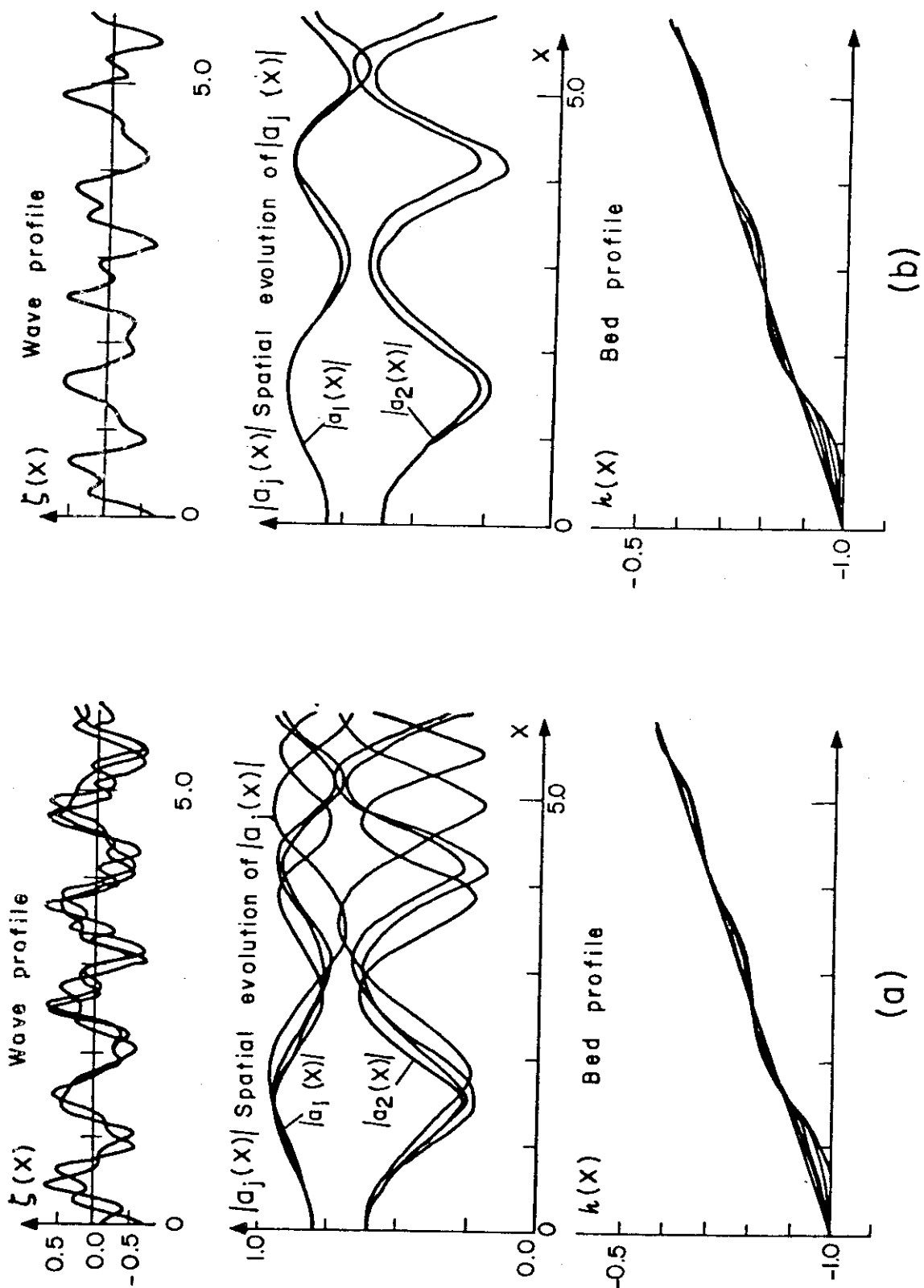


Figure 16.

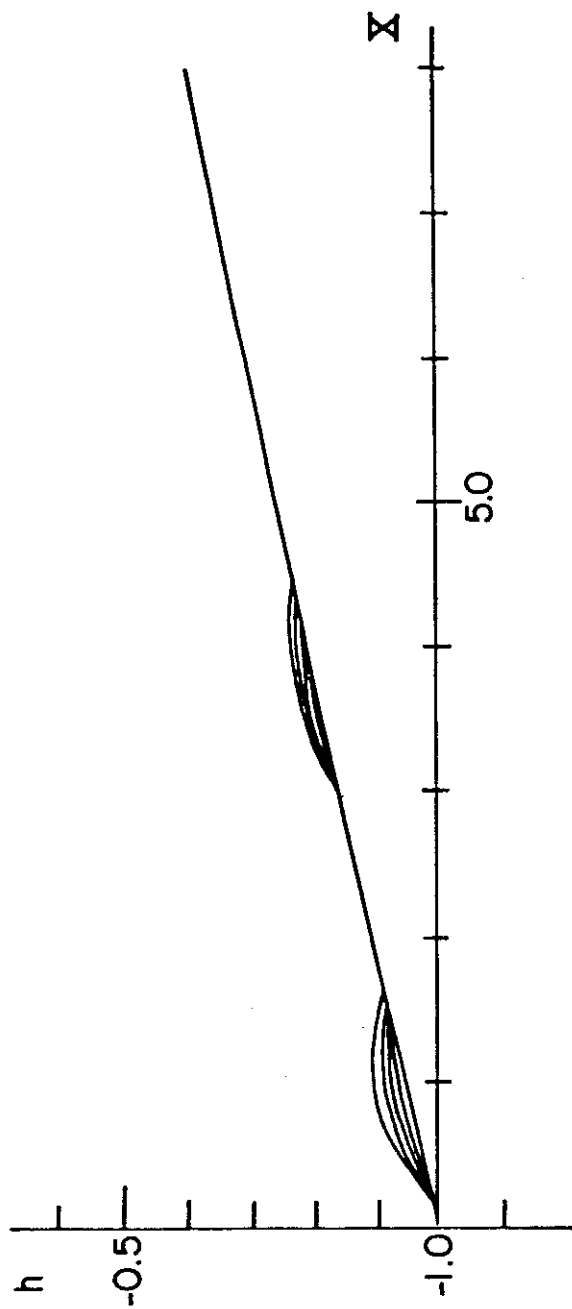
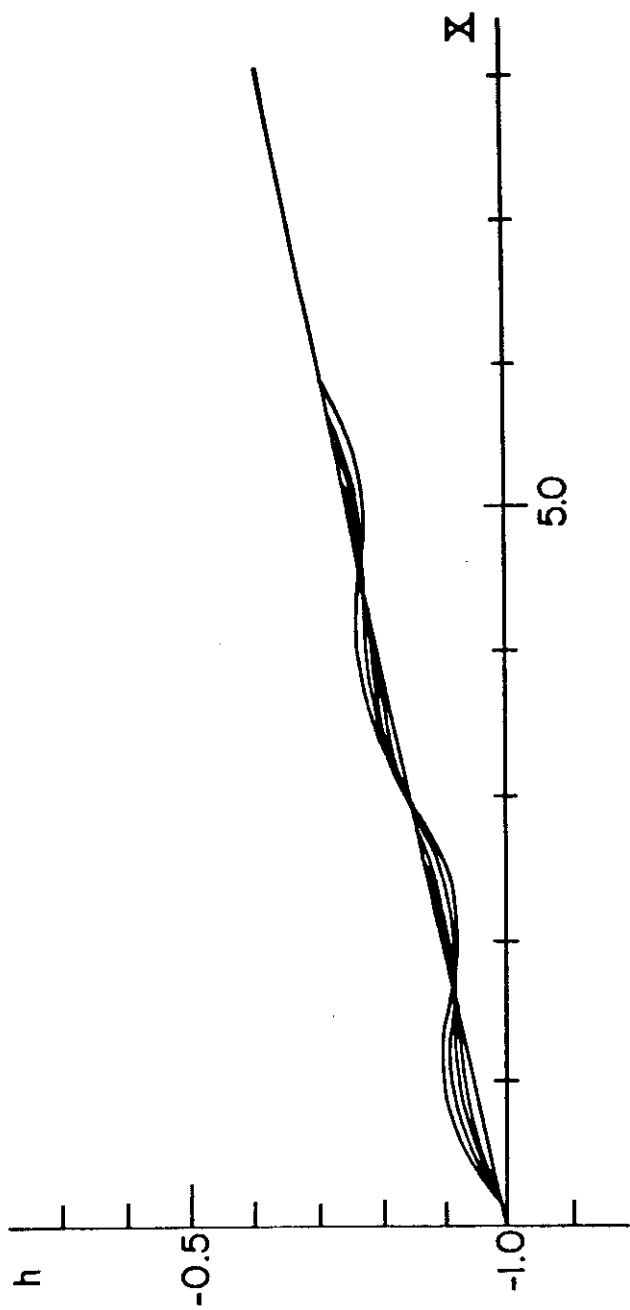


Figure 17.

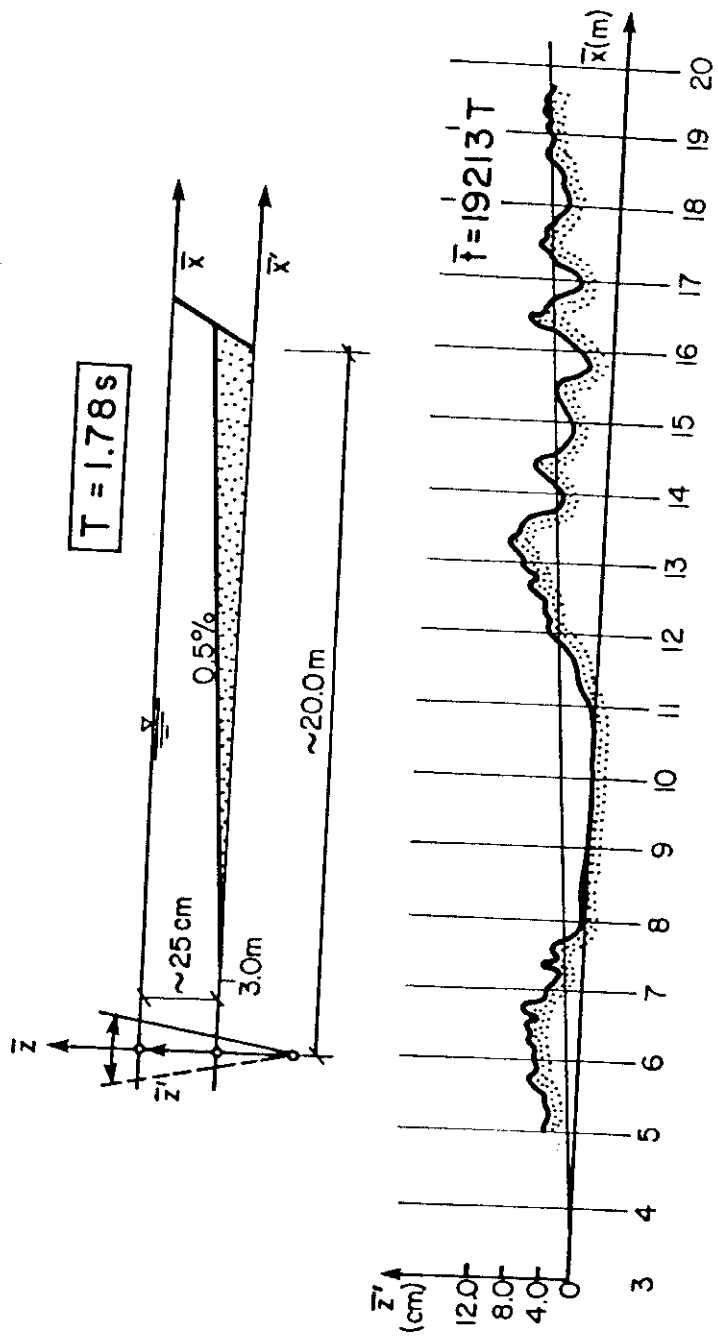


Figure 18.

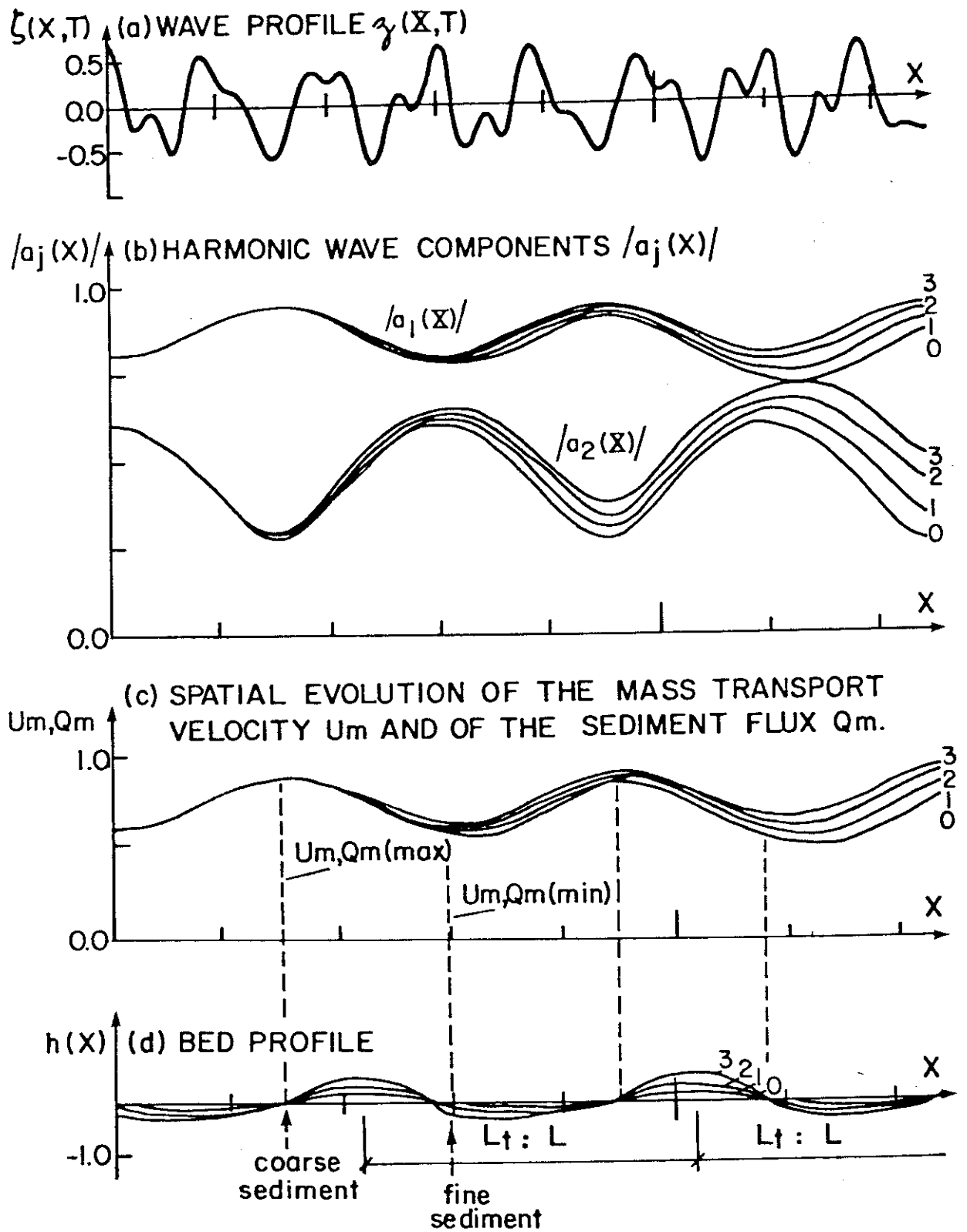


Figure 19.

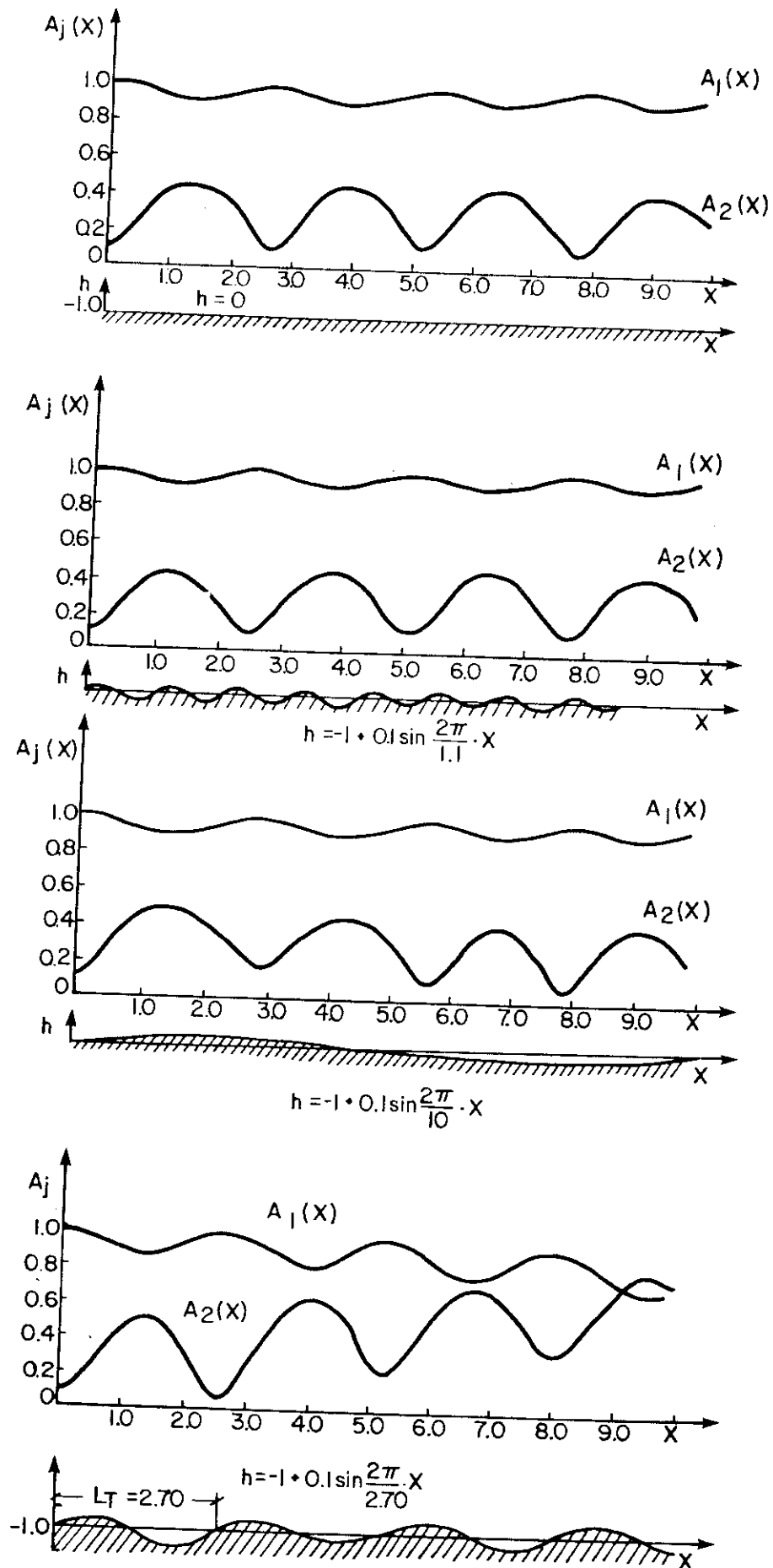


Figure 20.

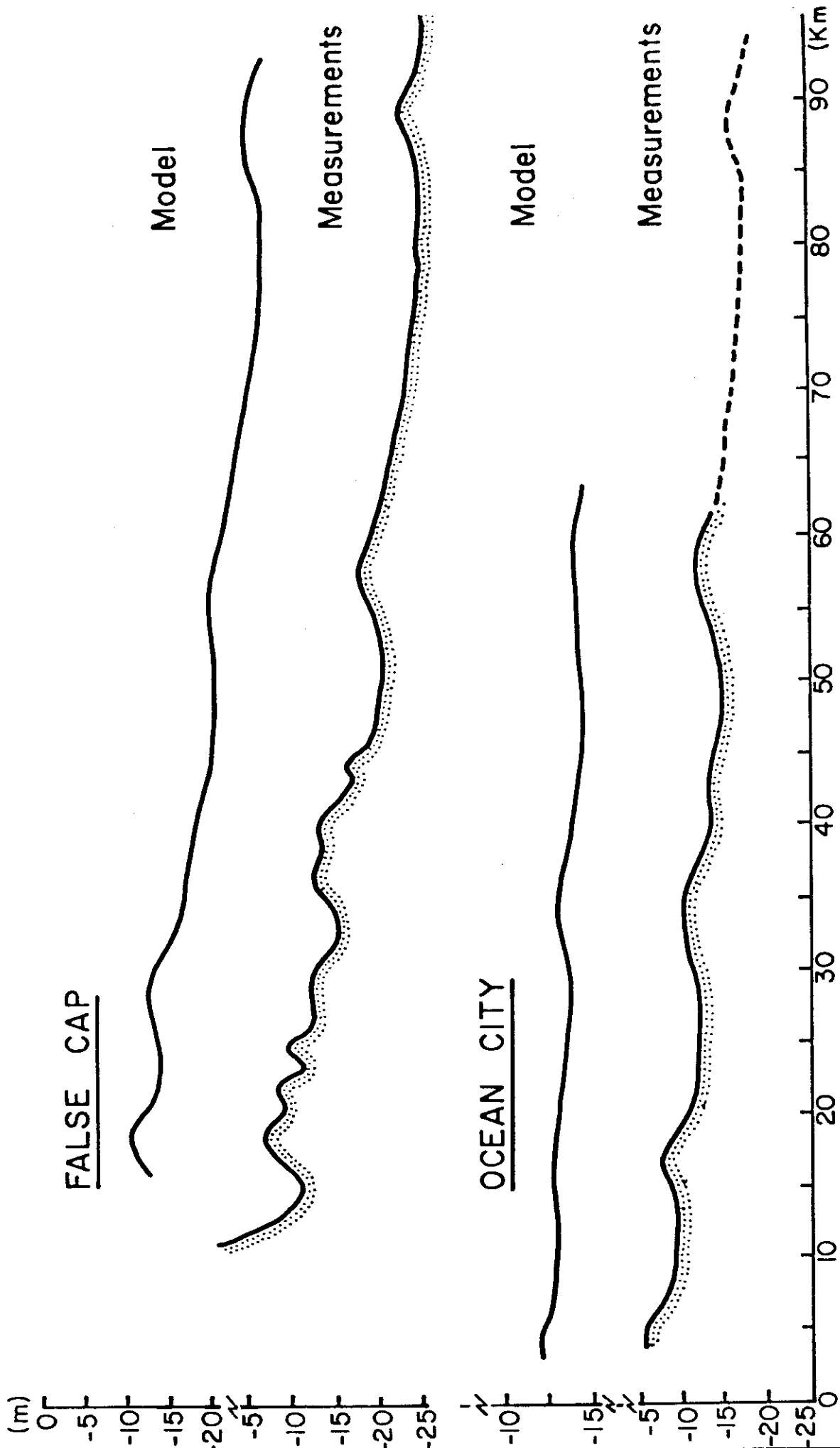


Figure 21.

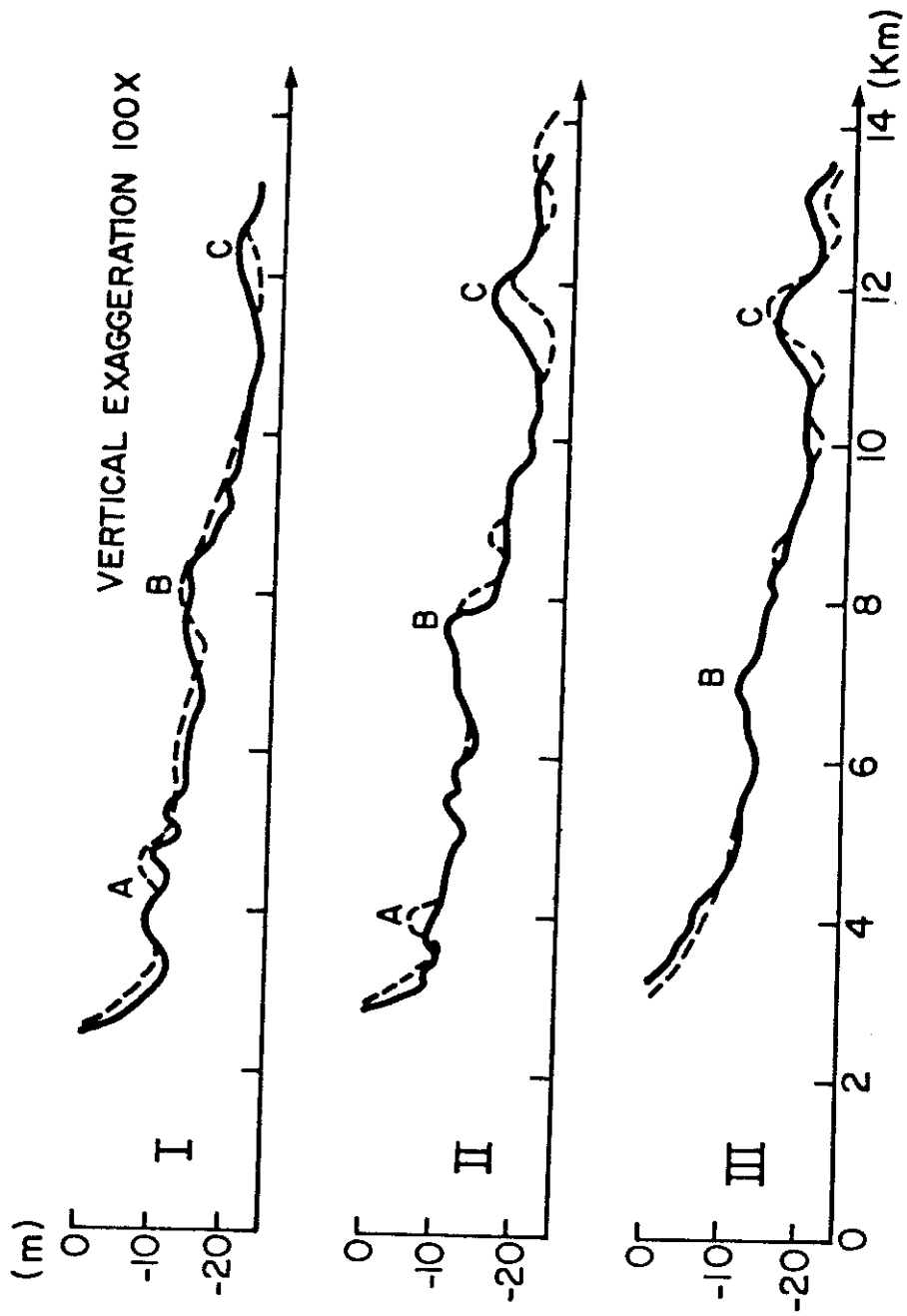


Figure 22.